

Integrating Probabilistic Trees and Causal Networks for Clinical and Epidemiological Data

Sheresh Zahoor^{a,*}, Pietro Liò^b, Gaël Dias^c, Mohammed Hasanuzzaman^d

^a*Munster Technological University, Rossa Ave, Bishopstown, Cork, Ireland*

^b*Department of Computer Science and Technology, University of Cambridge, The Old Schools, Trinity Ln, Cambridge, United Kingdom*

^c*Université Caen Normandie, ENSICAEN, CNRS, Normandie Univ, GREYC UMR6072, F-14000 Caen, France, Boulevard du Maréchal Juin, Caen, France*

^d*The School of Electronics, Electrical Engineering and Computer Science, Queens University Belfast, University Road, Belfast, United Kingdom*

Abstract

Healthcare decision-making requires not only accurate predictions but also insights into how factors influence patient outcomes. While traditional machine learning (ML) models excel at predicting outcomes, such as identifying high-risk patients, they are limited in addressing “what if” questions about interventions. This study introduces the Probabilistic Causal Fusion (PCF) framework, which integrates Causal Bayesian Networks (CBNs) and Probability Trees (PTrees) to extend beyond predictions. PCF leverages causal relationships from CBNs to structure PTrees, enabling both the quantification of factor impacts and the simulation of hypothetical interventions. PCF was validated on three real-world healthcare datasets i.e. MIMIC-IV, Framingham Heart Study, and Diabetes—chosen for their clinically diverse variables. It demonstrated predictive performance comparable to traditional ML models while providing additional causal reasoning capabilities. To enhance interpretability, PCF incorporates sensitivity analysis and SHapley Additive exPlanations (SHAP). Sensitivity analysis quantifies the influence of causal parameters on outcomes such as Length of Stay (LOS), Coronary Heart Disease (CHD), and Diabetes, while SHAP highlights the importance of individual features in predictive modeling. By combining causal reasoning with predictive modeling, PCF bridges the gap between clinical intuition and data-driven insights. Its ability to uncover relationships between modifiable factors and simulate hypothetical scenarios provides clinicians with a clearer understanding of causal pathways. This approach supports more informed, evidence-based decision-making, offering a robust framework for addressing complex questions in diverse healthcare settings.

Keywords: Causal Bayesian Networks, Healthcare, Probability Trees, Causal Inference

1. Introduction

Effective healthcare requires not just accurate predictions but also a deeper understanding of the factors that drive patient outcomes. While traditional machine learning (ML) models are proficient at identifying patterns and forecasting risks—such as predicting which patients are more likely to develop a condition—they often fall short in evaluating how specific interventions might alter these outcomes. This predictive focus limits their utility in addressing causal questions, such as estimating the impact of treatments or other modifiable factors on patient trajectories. To bridge this gap, there is a growing need for approaches that go beyond prediction, enabling the quantification of causal effects and simulation of intervention outcomes.

Causal ML addresses these gaps by estimating treatment effects and answering counterfactual questions, such as “How would a patient’s outcome change if a different treatment were administered?” Unlike traditional ML, which focuses on correlations, causal ML is built on the foundation of causal inference [1], enabling a deeper understanding of relationships and supporting evidence-based decision-making [2]. For instance, traditional ML might predict a patient’s likelihood of developing diabetes [3], but causal ML can estimate how that likelihood

would change under specific interventions, such as a lifestyle modification or a new medication [4]. These capabilities are particularly valuable in healthcare, where understanding cause-effect relationships is critical for developing targeted interventions [5].

To address these challenges, we propose the Probabilistic Causal Fusion (PCF) framework, which integrates Causal Bayesian Networks (CBNs) and ensembles of Probability Trees (PTrees) to bridge the gap between prediction and causality. CBNs use a directed acyclic graph (DAG) structure to model dependencies and causal pathways in healthcare data [2, 5, 6, 7], while PTrees offer an intuitive representation of probabilistic relationships, enabling reasoning about uncertainty and interactions between variables [8]. By combining these complementary approaches, PCF provides a powerful framework for understanding the relationships between factors and their impact on patient outcomes.

While Randomised Controlled Trials (RCTs) remain the gold standard for establishing causal relationships, they are often resource-intensive and ethically challenging. PCF offers an alternative by leveraging observational healthcare data to uncover causal relationships, quantify treatment effects, and simulate hypothetical interventions. Unlike traditional ML models, which focus on predicting outcomes based on correlations, PCF enables clinicians to explore the causal pathways underlying

*Corresponding author

Email address: sheresh.zahoor@mycit.ie (Sheresh Zahoor)

these outcomes and assess the effects of specific interventions.

The hierarchical structure of PCF enhances its clinical utility by leveraging the strengths of both CBNs and PTrees. CBNs investigate dependencies among morbidities and assess temporal relationships, while PTrees quantify the strength of these relationships across patient cohorts. This approach allows for the seamless integration of diverse data sources, such as clinical bedside information, into a unified framework for decision support. By using the causal knowledge derived from CBNs to structure the PTrees, PCF ensures that probabilistic dependencies reflect the underlying causal relationships in the data. This not only reduces the reliance on subjective domain expertise but also ensures consistency between the data and the model.

Traditionally, constructing PTrees has been an iterative process reliant on domain experts to define variable orderings [7], which introduces challenges such as:

1. **Subjectivity:** Expert knowledge may be incomplete or biased, leading to suboptimal structures.
2. **Inefficiency:** Manual construction is time-intensive, especially for complex datasets.
3. **Data Inconsistency:** Sole reliance on expert-defined structures can overlook key relationships present in the data.

By employing an ensemble learning approach, PCF mitigates these limitations, offering a robust and generalisable solution that reduces overfitting and enhances performance.

Beyond its modeling capabilities, PCF also establishes a centralised causal knowledge repository, fostering collaboration among healthcare institutions. Pre-trained PCF models, along with their underlying causal structures, can be shared across institutions, enabling smaller organisations to leverage collective expertise and refine models using their local data. This collaborative ecosystem ensures continuous improvement and supports the development of generalisable causal models that can address diverse healthcare challenges. Figure 1 summarises the steps involved in the proposed PCF framework.

In this work, we leverage the PCF framework to support prediction, intervention, and counterfactual analysis in three distinct clinical contexts. First, we aim to predict and identify factors associated with the length of stay in the Intensive Care Unit (ICU). Second, the framework is applied to assess the risk of Chronic Heart Disease (CHD) and investigate potential modifiable factors that could mitigate its progression. Finally, we utilise the framework to predict the risk of diabetes and analyse the influence of various risk factors on its onset.

The main contributions of this work are summarised as follows:

- We propose a framework, Probabilistic Causal Fusion (PCF), that combines Causal Bayesian Networks (CBNs) with ensembles of Probability Trees (PTrees) to enable predictions, interventions, and counterfactual analysis in healthcare. This integration addresses the limitations of traditional PTree construction, such as reliance on domain expertise for variable ordering, by leveraging causal relationships identified through CBNs.

- The use of an ensemble of PTrees improves predictive performance and robustness. By balancing the trade-off between bias and variance, the ensemble approach mitigates risks of overfitting or underfitting and enhances generalisability.
- Methodological refinements are introduced in computing transition probabilities within the PTree framework. Specifically, data is partitioned using empirical marginal probabilities, while causal relationships derived from CBNs inform split decisions, enabling more data-driven and effective model construction.
- The applicability and utility of the PCF framework are demonstrated through its application to multiple real-world healthcare datasets.

The structure of the paper is as follows. Section 2 provides an overview of the relevant literature, establishing the context and motivation for this work. Section 3 describes the proposed framework in detail, including the steps involved in its construction and implementation. Section 4 presents the application of the framework to three distinct clinical case studies, while Section 5 discusses the results obtained from these applications. Finally, Section 6 provides conclusive remarks and directions for future work.

2. Relevant Works

2.1. Traditional ML vs. Causal ML

Traditional ML has become a cornerstone in healthcare for tasks such as risk prediction, patient stratification, and outcome forecasting [9, 10]. These models are highly effective at identifying patterns and correlations, enabling predictions such as the likelihood of disease onset or hospital readmissions [11, 12, 13]. However, traditional ML lacks the ability to answer counterfactual questions or estimate treatment effects, as it is inherently focused on predictive accuracy rather than causal reasoning [14, 15].

In contrast, causal ML seeks to address "what if" questions by estimating the causal effect of interventions on outcomes. For instance, rather than simply predicting the probability of diabetes onset, causal ML can assess how this probability might change if a patient adopts a new medication or lifestyle modification [16, 17]. These capabilities enable healthcare providers to explore counterfactual scenarios and make data-driven decisions that go beyond prediction to inform treatment planning and resource allocation.

Causal ML requires additional considerations compared to traditional ML, such as the need to account for unobservable outcomes and confounding variables. For example, the "fundamental problem of causal inference" [18, 1] states that only factual outcomes under a given treatment are observed, while counterfactual outcomes remain unobserved. This poses challenges in estimating treatment effects and necessitates assumptions such as the absence of unmeasured confounders to ensure unbiased estimates. Additionally, causal ML models must account for the interconnectedness of variables, as interventions

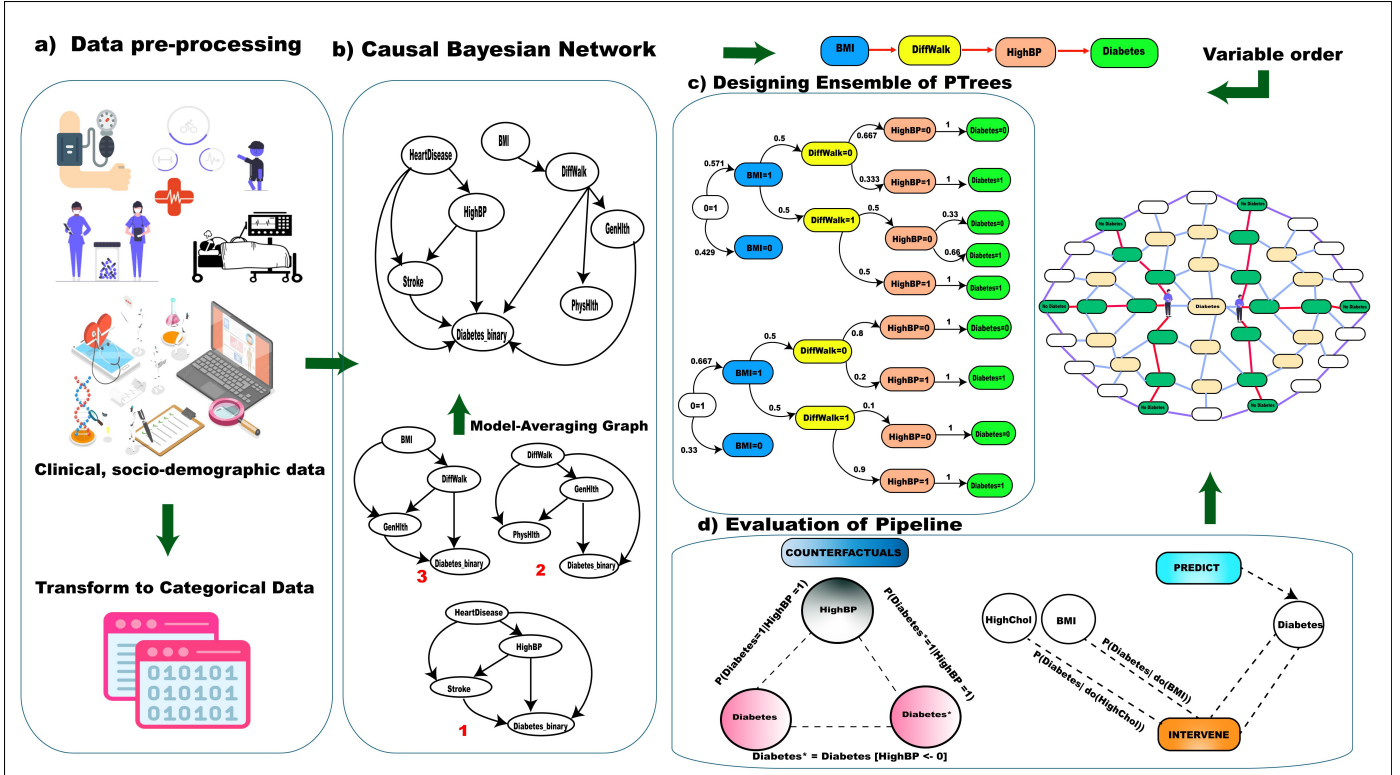


Figure 1: Different steps involved in the PCF framework. The first module addresses data pre-processing to shape the input required for the CBN. The next module involves generating individual CBNs and creating a model-averaging graph. Subsequently, the ensemble of PTrees is developed based on the variable order from the model-averaging graph. The final module involves evaluating the overall performance of PCF.

on one factor may influence others. For example, a smoking cessation intervention may indirectly affect diabetes risk through changes in body mass index (BMI), requiring a causal framework to model such dependencies.

2.2. Applications of CBNs in Healthcare

CBNs are a widely used tool in causal ML for modeling relationships among variables through a directed acyclic graph (DAG) structure. CBNs allow for the incorporation of prior knowledge and probabilistic reasoning, making them particularly effective for understanding complex dependencies in healthcare data. For instance, Rajendran et al. [19] employed CBNs to integrate risk factor analysis in breast cancer research, facilitating early detection and risk stratification. Shahmirzai et al. [20] applied CBNs to recurrent breast cancer data to predict survival outcomes and guide personalised treatment strategies. Similarly, Jang et al. [21] leveraged CBNs to model risks associated with radiation therapy, offering support for personalised oncology care.

CBNs have also been applied to explore relationships between cardiovascular risk factors and related conditions, as demonstrated by Ordoas et al. [22]. These examples highlight the versatility of CBNs in identifying risk factors, modeling disease progression, and simulating the effects of interventions. However, while CBNs excel at representing causal relationships, their construction often requires significant domain expertise and computational resources, which may limit scalability.

2.3. Probability Trees (PTrees) in Causal Modeling

Probability Trees (PTrees) offer an intuitive and sequential representation of probabilistic relationships. Grounded in probability theory, PTrees use a tree structure where each node represents a probabilistic event and branches correspond to the conditional probabilities of subsequent events [8]. This structure is particularly useful for modeling complex decision-making processes in healthcare, where uncertainty and sequential dependencies play a significant role.

Despite their simplicity and expressiveness, PTrees have received relatively less attention in the machine learning literature compared to CBNs or structural causal models. Ambags et al. [7] proposed a hybrid approach combining probabilistic fuzzy decision trees with causal reasoning, applying it in two medical case studies to demonstrate its potential for real-world applications. However, traditional PTree construction often relies on domain expertise for defining variable order, which can introduce subjectivity, inefficiency, and inconsistencies between expert-defined structures and data-driven insights.

By integrating PTree ensembles with causal insights derived from CBNs, frameworks like Probabilistic Causal Fusion (PCF) aim to address these limitations. The use of ensembles mitigates overfitting risks, while the causal order provided by CBNs ensures that the modeled relationships align with the underlying data-generating process.

2.4. Advances in Causal ML for Healthcare

Recent advances in causal ML demonstrate its potential for improving healthcare decision-making by estimating treatment effects and simulating counterfactual scenarios. These methods have been applied to a variety of clinical challenges, from estimating the effects of medication adherence on diabetes progression to predicting survival probabilities under different oncology treatment plans [5, 2]. By integrating causal ML techniques into clinical workflows, researchers aim to bridge the gap between prediction and actionable insights, enabling data-driven strategies for improving patient outcomes.

However, causal ML comes with its own challenges. Assumptions about unmeasured confounding, model scalability, and the reliability of observational data remain critical concerns [23]. Addressing these limitations through frameworks like PCF, which combine causal reasoning with robust predictive modeling, represents an important step toward leveraging causal ML in diverse healthcare contexts.

3. Methodology-PCF framework

This study introduces PCF, a novel framework combining the strengths of CBNs and PTrees for enhanced predictions, interventions, and counterfactual analyses. Traditionally, PTree construction involves selecting and ordering features based on domain expertise (deduction) and setting transition probabilities from empirical data (induction). This process is subjective and can impact model performance. Our framework leverages CBNs to autonomously determine the variable order, streamlining PTree construction and enhancing efficiency and accuracy. Additionally, forming an ensemble of multiple PTrees improves predictive performance by mitigating overfitting and underfitting through balancing bias and variance across diverse data subsets.

3.1. CBN Construction

CBNs are a powerful framework for elucidating the causal relationships among variables in complex datasets. In this phase, we utilised CBNs to reveal the causal architecture of selected variables and ascertain the optimal sequence in which they exert influence on the outcome variable Y . This sequencing is crucial for the subsequent development of a proficient Probability Tree (PTree). Given the set of variables $V = \{X_1, X_2, \dots, X_n\}$ and the outcome variable Y , we construct a Causal Bayesian Network (CBN) G such that:

- G represents the causal dependencies among the variables in V and Y .
- We identify a topological ordering of the variables that reflects the causal influence sequence leading to Y .

We employed the "target variable" knowledge approach from the Bayesys [24] open-source Bayesian Network Structure Learning (BNSL) system to prioritise structure learning to elucidate a greater number of parent nodes, revealing potential causal factors for the variable of interest i.e. Y

3.1.1. Methodological Steps

1. **Structure Learning:** For each algorithm A_i , we aim to find the optimal network structure G_i that maximises a given scoring function S . The algorithms used include Hill Climbing (HC) [25, 26], TABU [27], SaiyanH [28], Model-Averaging Hill-Climbing (MAHC) [29], and Greedy Equivalence Search (GES) [30] The optimal structure G_i is determined by:

$$G_i = \arg \max_G S(G | \text{data})$$

These algorithms were chosen for their capability to incorporate the target variable during model construction and to handle diverse knowledge approaches, including direct relationships and forbidden edges [31].

2. **Model Averaging:** To address the biases and limitations of individual algorithms, we adopted the model-averaging strategy implemented in Bayesys [24] to combine multiple structures G_i into an averaged graph G_{avg} . The following steps outline this process:

- a. **Directed Edges:** Add directed edges $e = (u, v)$ to G_{avg} starting with the edges that occur most frequently across input graphs, ensuring no cycles are formed:

$$e \in G_{\text{avg}} \text{ if } \text{freq}(e) > \text{threshold and no cycle}$$

If adding an edge e would create a cycle, reverse the edge:

$$e \rightarrow e^{-1} \text{ if } e \text{ forms a cycle}$$

- b. **Undirected Edges:** Add undirected edges $e = \{u, v\}$ to G_{avg} , skipping those already added as directed edges:

$$e \in G_{\text{avg}} \text{ if } \text{freq}(e) > \text{threshold}$$

- c. **Cycle Handling:** Add directed edges from the cycle-inducing edge set C :

$$e \in G_{\text{avg}} \text{ if } e \in C \text{ and occurs frequently}$$

By employing this model-averaging approach, we create a single Directed Acyclic Graph (DAG) that consolidates insights from all considered structure learning algorithms. This enhances the robustness and reliability of the learnt graph, mitigating algorithmic biases and addressing limitations in edge orientation from observational data.

3. **Topological Sorting:** Determine a topological order π of the nodes in G_{avg} . This ordering is crucial for ensuring that the nodes are processed in a sequence that respects the causal dependencies:

$$\pi = \text{topological_sort}(G_{\text{avg}})$$

The sorted order π is then used in the construction of PTrees, facilitating their development and enhancing their predictive capabilities.

3.1.2. Sensitivity Analysis

Sensitivity analysis is performed to assess the responsiveness of nodes to changes in their parent and ancestor nodes [32]. For a node X_i with parent X_j , sensitivity S is defined as:

$$S = \frac{\partial P(X_i)}{\partial \theta_{X_j}}$$

where θ_{X_j} represents the parameters in the Conditional Probability Table (CPT) of X_j . High sensitivity indicates that small changes in θ_{X_j} result in significant changes in the posterior distribution of X_i , suggesting a strong dependency. Conversely, low sensitivity implies that large changes in θ_{X_j} have minimal impact on X_i 's distribution, indicating a weak dependency.

The posterior probability T of the selected state of the target node, given the parameter p , is represented by the following general linear rational functional form:

$$T = \frac{a \cdot p + b}{c \cdot p + d}$$

The sensitivity analysis algorithm calculates the coefficients a, b, c , and d . The derivative, which is the basic measure of sensitivity, is given by:

$$D = \frac{a \cdot d - b \cdot c}{(c \cdot p + d)^2}$$

The denominator is positive, indicating that the sign of the derivative is constant for all values of p . By substituting 0 and 1 for p (noting that p is a probability), we can calculate the range within which the posterior will change if p is modified across its entire range, defined by:

$$p_1 = \frac{b}{d}$$

$$p_2 = \frac{a + b}{c + d}$$

Sensitivity analysis is crucial in understanding the stability and robustness of the model. It helps identify the most influential parameters in the network, guiding targeted interventions and enhancing the interpretability of the model. We use the GeNIe BN software [33] to perform this analysis.

3.2. Probability Tree Construction

Based on the CBN framework, we construct Probability Trees (PTrees) as follows:

3.2.1. Create Tree from Data

The process commences with Algorithm 1 (CREATE_TREE_FROM_DATA), which outlines the construction of a PTree from a given dataset and the variable order derived from the previously learned CBN.

- a. Construct a PTree T from dataset D using the variable order π derived from the CBN G .
- b. **Root Level:** Partition data based on the prevalent value of the target attribute Y :

$$p(v) = \frac{\text{Count}(v)}{\text{Total Samples}}$$

where:

- $p(v)$ denotes the initial probability for a given value v of Y .
- $\text{Count}(v)$ is the number of occurrences of v in Y .
- Total Samples is the total number of samples.

This initial partitioning uses empirical marginal probabilities to establish a foundation for the tree structure.

- c. **Transition Probabilities:** Calculate transition probabilities using the causal structure:

$$P(X_{\text{current}} | X_{\text{parent}}) = \frac{\text{Count}(X_{\text{current}}, X_{\text{parent}})}{\text{Count}(X_{\text{parent}})}$$

where:

- $P(X_{\text{current}} | X_{\text{parent}})$ represents the transition probability of the current attribute given the parent attribute.
- $\text{Count}(X_{\text{current}}, X_{\text{parent}})$ denotes the number of occurrences of the current value given the parent value.
- $\text{Count}(X_{\text{parent}})$ represents the total number of occurrences of the parent value.

This context-aware approach leverages the parent-child relationships identified by the CBN, enabling the tree to make more precise and informed splits, thereby potentially enhancing its predictive capabilities.

- d. **Pruning:** Employ pruning to prevent overfitting by evaluating conditional probabilities against a threshold. Only branches with probabilities exceeding this threshold are retained, ensuring the tree focuses on the most significant splits.

3.2.2. Ensemble Learning

A key innovation of our proposed method is the use of ensemble learning to build a robust prediction model. This approach enhances the reliability and accuracy of the predictions. The ensemble learning process within our framework is implemented through the ENSEMBLE_PROBABILITY_TREES function, which follows a three-step strategy:

- a. **Data Splitting:** Divide D into k distinct subsets $\{D_1, D_2, \dots, D_k\}$.
- b. **Diverse PTrees:** Construct a PTree T_i for each subset D_i using Algorithm 1 CREATE_TREE_FROM_DATA:

$$T_i = \text{CREATE_TREE_FROM_DATA}(D_i, \pi)$$

- c. **Root Node Storage:** Store root nodes of individual PTrees in a list `ptrees`.

3.2.3. Prediction Process

To leverage the ensemble of PTrees for making predictions, we follow these steps:

- a. **Individual Predictions:** For each PTree T_i , generate a prediction \hat{y}_i for a given data point using the Predict function. This step utilises the structure and relationships captured within each tree to produce a prediction:

$$\hat{y}_i = \text{Predict}(T_i, \text{data point})$$

Each tree in the ensemble provides its own prediction, reflecting the diverse insights each tree has gained from its subset of the data. As an integral component of the predictive framework, Algorithm 2 calculates the conditional probability of a specified class based on a defined set of input conditions.

- b. **Averaging Predictions:** Combine the predictions from all k PTrees by calculating the average prediction. This step helps to smooth out individual tree biases and improve overall predictive accuracy:

$$\hat{y}_{\text{avg}} = \frac{1}{k} \sum_{i=1}^k \hat{y}_i$$

The averaged prediction \hat{y}_{avg} provides a consensus estimate, leveraging the collective knowledge of the entire ensemble.

- c. **Threshold Classification:** Classify data points based on the averaged prediction using a predefined threshold τ . This classification step assigns a final class label, determining whether the data point belongs to the positive or negative class:

$$\text{Class} = \begin{cases} \text{Positive} & \text{if } \hat{y}_{\text{avg}} > \tau \\ \text{Negative} & \text{if } \hat{y}_{\text{avg}} \leq \tau \end{cases}$$

The threshold τ can be adjusted depending on the specific requirements of the application, allowing for flexible decision-making.

By incorporating predictions from this diverse ensemble of PTrees, the model comprehensively understands the complex relationships within the data, thereby enhancing its predictive capabilities.

3.2.4. SHapley Additive exPlanations (SHAP)

To enhance model interpretability and elucidate feature importance, SHAP [34] was integrated into the framework. SHAP values provide a unified measure of feature importance, enabling us to understand the contribution of each feature to the model's predictions. This enhances the transparency and trustworthiness of our model's outputs. Rooted in cooperative game

theory, SHAP values offer a method to attribute the difference between the prediction for a specific instance and the average prediction to individual features. SHAP values adhere to local accuracy, missingness, and consistency, ensuring reliable and interpretable explanations. Mathematically, for a model f and an instance x , the SHAP value ϕ_i for feature i is calculated as:

$$\phi_i = \sum_{S \subseteq N \setminus \{i\}} \frac{|S|!(|N| - |S| - 1)!}{|N|!} [f(S \cup \{i\}) - f(S)]$$

where:

- N is the set of all features.
- S is a subset of N that excludes feature i .
- $f(S)$ is the prediction for the instance with only the features in S .

This formula calculates the average marginal contribution of feature i across all possible feature subsets, ensuring fair and comprehensive feature importance attribution.

To facilitate SHAP analysis, predictions from the ensemble of PTrees were encapsulated in a wrapper compatible with the SHAP framework. A background dataset was generated using k-means clustering on the training data to provide a reference point for SHAP value calculations. SHAP values were computed for a subset of the test data using the Kernel Explainer to balance computational efficiency and accuracy

4. Case Studies

The proposed framework addresses several limitations of traditional prediction models by offering a multifaceted approach for clinicians. It facilitates the identification of causal relationships between variables, enables predictive modeling, and supports the exploration of potential interventions and counterfactual scenarios. This combination provides clinicians with a more comprehensive understanding of the data while acknowledging the inherent challenges of causal analysis.

We evaluated the framework using multiple real-world healthcare datasets to assess its applicability and generalisability across diverse clinical contexts. The first dataset was MIMIC-IV, a collection of electronic health records from critical care settings, where the objective was to predict the length of stay in the Intensive Care Unit (ICU). The second dataset was the Framingham Heart Study, which focuses on cardiovascular disease (CVD) and its risk factors, trends over time, and familial patterns. Finally, the Diabetes dataset from BRFSS-2015 was used to analyse risk factors and predict the likelihood of diabetes onset. These case studies were selected to evaluate the framework's utility in diverse scenarios and assess its ability to handle distinct clinical challenges.

4.1. Length of stay in ICU case study

The intensive care unit (ICU) stands as a vital line of defense for critically ill patients, offering specialised care to prevent deterioration from severe illness or injury [35], [36]. However,

Algorithm 1 Create Tree from Data

Require: *father_node*: Node, *data*: DataFrame, *variable_order*: List, *level*: Integer, *pruning_threshold*: Float

Ensure: Root node of the decision tree (*father_node*)

```
1: function CREATE_TREE_FROM_DATA(father_node, data,  
  variable_order, level, pruning_threshold)  
2:   current_variable  $\leftarrow$  variable_order[0]  
3:   current_data  $\leftarrow$  data[current_variable]  
4:   class_nodes  $\leftarrow$  empty list  
5:   for val in unique values of current_data do  
6:     Create class node with ID, level, statements, and no  
     children  
7:     Append class node to class_nodes  
8:   end for  
9:   total_samples  $\leftarrow$  total number of samples in  
     current_data  
10:  for each class_node and val in class_nodes do  
11:    is_root  $\leftarrow$  Check if father_node is root  
12:    val_count  $\leftarrow$  Count of val in current_data  
13:    if is_root then  
14:      Calculate transition probability based on occur-  
     rences  
15:      if transition_prob  $\geq$  pruning_threshold then  
16:        Insert transition probability into  
        father_node  
17:      end if  
18:    else  
19:      Calculate transition probability based on par-  
     ent's state  
20:      if transition_prob  $\geq$  pruning_threshold then  
21:        Insert transition probability into  
        father_node  
22:      end if  
23:    end if  
24:  end for  
25:  for each class_node and val in class_nodes do  
26:    Get next data for val  
27:    Get next variable order  
28:    if next variable order is not empty then  
29:      Recursively call create_tree_from_data  
30:    end if  
31:  end for  
32:  return father_node  
33: end function
```

Algorithm 2 Conditional Probability Calculation

```
1: function CONDITIONALPROBABILITY(self, input_condition)  
2:   if input_condition is empty then  
3:     return 0.0  
4:   end if  
5:   cut_disease  $\leftarrow$  self.prop('target_variable')  
6:   combined_cut  $\leftarrow$  None  
7:   for all (var, val) in input_condition do  
8:     cut  $\leftarrow$  self.prop(var + ' = ' + val)  
9:     if combined_cut is None then  
10:      combined_cut  $\leftarrow$  cut  
11:    else  
12:      combined_cut  $\leftarrow$  combined_cut  $\wedge$  cut  
13:    end if  
14:  end for  
15:  disease_see  $\leftarrow$  self.see(combined_cut)  
16:  probability  $\leftarrow$  disease_see.prob(cut_disease)  
17:  return probability  
18: end function
```

the ever-increasing demand for ICU beds threatens this critical service. The imbalance between ICU capacity and patient needs has significant consequences for patient outcomes, public health, and even socio-economic factors [37], [38]. Therefore, optimising ICU resource allocation and planning for future needs necessitates interpretable models that facilitate counterfactual analysis for informed decision-making, ultimately ensuring optimal care for critically ill patients.

4.1.1. MIMIC-IV

In this study, we use the MIMIC-IV version 2.2 database [39], which includes patients admitted to the BETH Israel Deaconess Medical Center during the period 2008–2019. The data contains multiple dimensions, from administrative data to laboratory results and diagnoses. We employed preprocessing techniques as described in [40] to ensure consistency and comparability with existing literature. The cohort included all patients with at least one ICU visit. However, certain subsets of patients were excluded: those who died during their ICU stay, those who returned to the ICU within 48 hours of discharge, those with an LOS greater than 21 days, and those with an LOS of less than one day.

The exclusion of patients who returned to the ICU within 48 hours was motivated by the focus of this analysis on understanding factors influencing the initial ICU stay and its length. Rapid readmissions often reflect distinct cases with underlying complexities such as incomplete recovery or premature discharge, which could introduce confounding factors. Similarly, patients with extremely long LOS (greater than 21 days) were excluded to avoid the influence of outliers, which could disproportionately impact model performance. Patients with an LOS of less than one day were excluded because the data collected during the first 24 hours was used for modeling, making such cases incomplete for analysis. These exclusions ensure that the cohort is representative of the broader ICU patient population,

allowing for more generalisable findings. Future work could investigate the effects of these exclusions on model performance by reintroducing these subsets for a comparative analysis.

To transform the length-of-stay task into a classification problem, we categorised LOS into clinically meaningful groups: short stays (1–4 days) and long stays (greater than 4 days). This categorisation was guided by the 75th percentile of LOS distribution ($Q3 = 4.0$) in the dataset, as described in [40], and reflects thresholds commonly used in critical care practice.

4.2. Heart Disease case study

Despite significant advancements in healthcare, CHD remains a leading cause of global mortality, accounting for 17.9 million deaths in 2019 as reported by the World Health Organization (WHO) [41]. While accurate prediction of future risk is undeniably crucial, medical experts increasingly recognise the limitations of solely relying on such prognostic models. To optimise patient care, a deeper understanding of the factors influencing individual susceptibility to CHD is paramount. This necessitates the development of intelligent systems that can not only predict future risk but also explore the potential impact of interventions and counterfactual analysis.

4.2.1. Framingham Data

In this study, we use the Framingham heart disease dataset includes over 4238 records and 15 attributes [42]. The goal of the dataset is to predict whether the patient has 10-year risk of future CHD. The initial preprocessing steps involved converting the numerical variables in the dataset into categorical variables. Given that the variables pertain to health-related data, specific ranges were meticulously considered during this conversion process. Numerical data representing health metrics such as blood pressure, cholesterol levels, or body mass index were categorised into clinically relevant ranges indicative of different health conditions or risk levels. By transforming numerical data into categorical form based on meaningful health-related ranges, the dataset became better suited for subsequent analysis and interpretation within the context of healthcare applications.

4.3. Diabetes case study

Despite the existence of preventative measures, diabetes remains a significant global health burden [43]. Characterised spectrum of devastating complications, it necessitates a multifaceted approach that transcends traditional risk prediction. While accurate future risk prediction remains valuable for preventative strategies, a deeper understanding of modifiable factors influencing individual susceptibility is paramount, especially considering the potential for early intervention to reduce diabetes-related mortality [44]. This necessitates the development of robust computational models capable of not only predicting future risk but also exploring the potential impact of various interventions through counterfactual analysis. Such models could empower clinicians by enabling the exploration

of "what-if" scenarios: investigating how a patient's risk profile might change with different lifestyle modifications or therapeutic interventions, ultimately leading to tailored preventative strategies and optimised patient care.

4.3.1. Diabetes Data

Data was obtained from the Behavioral Risk Factor Surveillance System (BRFSS), which is the primary system of health-related telephone surveys that collect state data on risk behaviours, chronic health conditions, and use of preventative treatments amongst U.S. residents [45]. The survey started in 1984 and currently performs over 400,000 adult interviews each year, making it the world's largest continuously conducted health survey system. This survey data provides a dataset that could be used to analyse and forecast diabetes risk variables. We utilised the BRFSS-2015 dataset, which included 253,680 health assessments.

5. Evaluation and discussion of the results

The evaluation process begins in Section 5.1 with an analysis of the varying outcomes derived from the sensitivity analysis. In Section 5.2, we assess the predictive performance of the PCF model, comparing it against a range of benchmark models, including both interpretable and non-interpretable methods, across all three datasets. Additionally, this section explores model interpretability using SHAP. Section 5.3 then examines the effects of potential interventions through interventional analysis. Lastly, Section 5.4 investigates counterfactual analysis to provide further insights.

5.1. Interpretation of Sensitivity Analysis

Sensitivity analysis is a crucial step in our framework to understand the influence of various parameters on the target variable. The diverse outcomes from our sensitivity analysis provide valuable insights into the multifaceted factors influencing LOS, CHD, and Diabetes, as depicted in Figure 2. The color of the bars indicates the direction of change in the target state, with red representing a negative impact and green representing a positive impact. For LOS, factors such as first care unit admission, patient's verbal communication ability, and specific diagnoses (e.g., Respiratory system, Circulatory system) show high sensitivity, indicating their collective substantial impact on LOS. In the context of CHD, the absence of diabetes and hypertension was found to significantly reduce the risk. Additionally, other significant factors include being a non-smoker with normal systolic blood pressure and specific education levels. These findings highlight the combined effect of lifestyle and socio-economic factors on CHD risk. For Diabetes, the sensitivity analysis demonstrates the complex interplay between hypertension, cholesterol levels, BMI, and other health indicators. The figure reveals that individuals with hypertension have the highest sensitivity value, indicating that high blood pressure significantly increases the risk of developing diabetes. Additionally, other influential factors include high cholesterol, elevated BMI, and the presence of heart disease. These findings underscore

the complex interplay of multiple health conditions in determining diabetes risk, highlighting the necessity of addressing various health parameters simultaneously to effectively manage and prevent diabetes.

5.2. Prediction

This section evaluates the predictive capabilities of PCF by applying it to three clinical datasets. We conduct a comprehensive assessment of its performance by juxtaposing its outcomes against those attained by established benchmark methodologies, comprising Logistic Regression (LR) [46], Decision Tree (DT) [47], Random Forest (RF) [48], Support Vector Machine (SVM) [49], K-Nearest Neighbors (KNN)[50], [51], Gradient Boosting (GB) [52], [53], eXtreme Gradient Boosting (XGB) [54], and Adaptive Boosting (Adaboost) [55]. Noteworthy among these benchmarks are LR, DT, and KNN, esteemed for their interpretability, which facilitates the elucidation of their decision-making mechanisms. Additionally, given the ensemble nature of our approach involving PTrees, a comparison with ensemble techniques such as GB, XGB, Adaboost and RF is warranted.

The dataset undergoes stratification-based partitioning into training and testing subsets to ensure their representativeness. Subsequently, the performance of each model is assessed utilising diverse metrics such as accuracy, specificity, sensitivity, and the Area Under the Receiver Operating Characteristic Curve (AUC-ROC). Predictions are made based on a default threshold, with the potential for adjustment in scenarios characterised by resource constraints, thereby prioritising cases of utmost urgency.

The performance metrics for each dataset are presented in Table 1, 2 and 3. It is well-documented that class imbalance within datasets can significantly impact the evaluation of machine learning algorithms. To mitigate this potential bias and ensure a fair comparison across all models, various techniques for handling class imbalance were employed. In the case of the MIMIC-IV and Framingham heart datasets, the SMOTE (Synthetic Minority Over-Sampling Technique) [56] oversampling technique yielded superior results. Conversely, ADASYN (Adaptive Synthetic Minority Oversampling Technique) [57] demonstrated the best performance when applied to the diabetes dataset. This finding suggests that the most effective class imbalance handling technique may vary depending on the specific characteristics of the data and the machine learning models being evaluated.

Tables 1, 2, and 3 present the performance evaluation of the PCF framework compared to benchmark methodologies across the three datasets. Notably, PCF achieves results that are largely comparable to established ensemble-based and interpretable models, balancing specificity and sensitivity while maintaining competitive predictive accuracy.

On the MIMIC-IV dataset, PCF achieves an accuracy of 73.21% and an AUC-ROC of 67.13%, performing similarly to ensemble-based methods such as Gradient Boosting (73.71% accuracy) and Adaboost (75.07% accuracy). Although DT achieves a higher accuracy of 79.42%, PCF demonstrates better sensitivity (56.56%) than simpler models like KNN, which

Table 1
Results using SMOTE for MIMIC-IV

Algorithm	Accuracy	Specificity	Sensitivity	AUC-ROC
Ensemble Algorithms				
GB	73.71	77.96	57.91	67.94
XGB	73.92	79.14	54.54	66.84
Adaboost	75.07	79.78	57.57	68.67
RF	75.64	83.22	47.47	65.35
PCF	73.21	77.69	56.56	67.13
Other Algorithms				
SVM	73.07	76.42	60.60	68.51
KNN	71.14	77.87	46.12	62.00
Interpretable Algorithms				
DT	79.42	88.84	44.44	66.64
LR	70.14	73.70	56.90	65.30
PTree	80.29	91.11	40.06	65.59

Table 2
Results using SMOTE for Framingham heart data

Algorithm	Accuracy	Specificity	Sensitivity	AUC-ROC
Ensemble Algorithms				
GB	63.08	64.81	53.48	59.15
XGB	63.91	68.01	41.08	54.54
Adaboost	66.03	69.26	48.06	58.66
RF	67.09	72.73	35.65	54.19
PCF	66.98	69.68	51.93	60.80
Other Algorithms				
SVM	69.22	74.26	41.08	57.67
KNN	76.76	87.62	16.27	51.95
Interpretable Algorithms				
DT	64.03	66.06	52.71	59.38
LR	61.55	63.14	52.71	57.92
PTree	65.57	70.23	39.53	54.88

achieves only 46.12%. Among ensemble methods, PCF effectively balances specificity and sensitivity, avoiding extremes like RF, which prioritises specificity at the expense of sensitivity.

On the Framingham dataset, PCF achieves an AUC-ROC of 60.80%, outperforming most ensemble methods while maintaining competitive accuracy at 66.98%, compared to RF (67.09%) and Adaboost (66.03%). Although KNN achieves the highest accuracy at 76.76%, its significantly lower sensitivity (16.27%) highlights its limitations in handling balanced classification scenarios. PCF’s balanced trade-off between specificity and sensitivity makes it particularly well-suited for datasets requiring nuanced predictions.

On the diabetes dataset, PCF achieves the highest AUC-ROC among all models (74.27%) and an accuracy of 73.64%, comparable to ensemble methods such as RF (73.42%) and higher than DT (62.92%). While KNN achieves the highest accuracy (79.00%), its specificity (85.86%) comes at the cost of sensitivity (35.26%). PCF balances both metrics effectively, achieving 73.41% specificity and 75.13% sensitivity, demonstrating its robustness across diverse datasets.

Overall, while PCF does not consistently outperform simpler models such as DT or KNN in terms of accuracy, it offers balanced performance across key metrics and demonstrates robustness across datasets. Its ability to maintain competitive predictive performance while also uncovering causal relationships and supporting intervention modeling sets it apart from purely predictive methodologies.

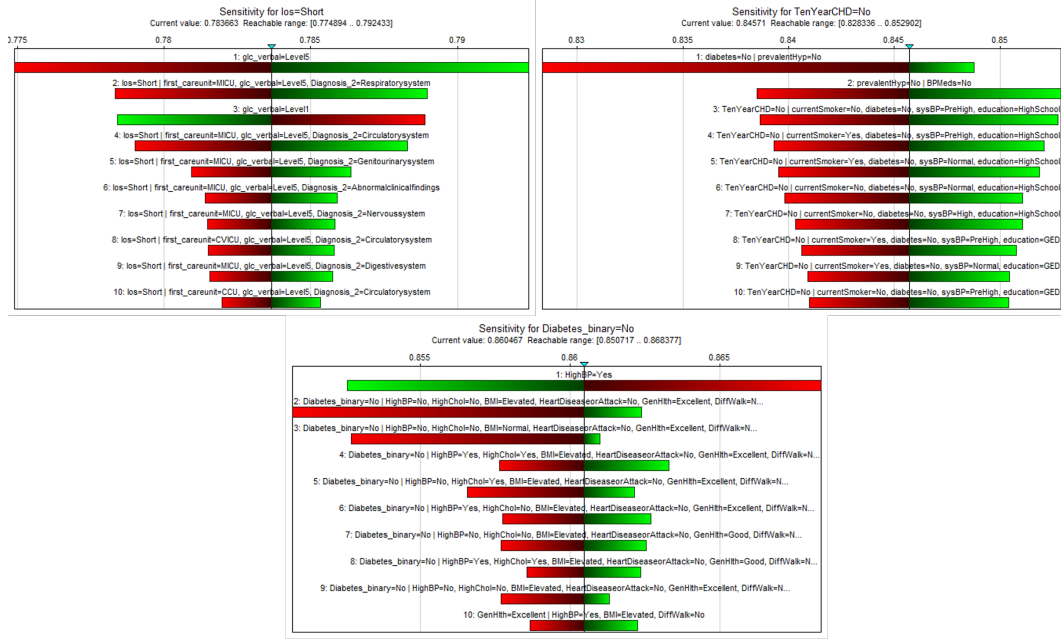


Figure 2: Sensitivity Analysis for LOS, Diabetes, and Framingham datasets.

Table 3
Results using ADASYN for diabetes data

Algorithm	Accuracy	Specificity	Sensitivity	AUC-ROC
Ensemble Algorithms				
GB	70.78	70.02	75.66	72.84
XGB	69.71	71.34	59.25	65.30
Adaboost	71.35	71.09	73.01	72.05
RF	73.42	77.45	47.61	62.53
PCF	73.64	73.41	75.13	74.27
Other Algorithms				
SVM	69.71	68.62	76.71	72.67
KNN	79.00	85.86	35.26	60.56
Interpretable Algorithms				
DT	62.92	60.19	80.42	70.31
LR	70.71	70.27	73.54	71.90
PTree	72.36	71.12	52.82	61.97

5.2.1. Interpretability with SHAP

The SHAP plot, shown in Figure 3, interprets the influence of each feature on predictions for LOS, Coronary Heart Disease (CHD), and Diabetes. For LOS, features such as creatinine, first care unit, and urea nitrogen have high SHAP values, indicating their strong influence on prolonged ICU stays. The Glasgow Coma Scale (gic_verbal) score and elevated white blood cells, along with specific diagnoses (e.g., respiratory and circulatory system issues), also significantly impact LOS predictions. In CHD predictions, critical features include current smoking status, systolic blood pressure (sysBP), and glucose levels, which are known risk factors for heart disease. High cholesterol (totChol), the presence of diabetes, socio-economic factors, and lifestyle choices such as education level and physical activity further influence CHD risk. For Diabetes, key contributors include high blood pressure (HighBP), elevated BMI, and high cholesterol levels, which are essential components of metabolic syndrome. General health status (GenHlth) and difficult walking (DiffWalk) also play significant roles, along with

the presence of heart disease and levels of physical activity. The SHAP plots reveal that LOS is heavily influenced by clinical indicators related to critical health conditions and specific ICU units. CHD risk is predominantly affected by cardiovascular risk factors, lifestyle choices, and socio-economic factors, while Diabetes risk is determined by metabolic health markers, overall health, and physical activity. These insights validate the results from sensitivity analysis and provide a detailed understanding of feature contributions, helping identify key areas for intervention and improve clinical decision-making processes by emphasising the most impactful factors for each health condition. By combining sensitivity analysis for understanding variable influence within the CBN and SHAP values for detailed prediction explanations, our framework ensures robust causal inference and clear, actionable insights for clinical decision-making.

5.3. Intervention

In the context of PCF, intervention involves the strategic modification of transition probabilities to ensure a specific event occurs with certainty (probability of 1). This approach allows for the exploration of conditional probabilities represented as $P(A|do(B))$, indicating the probability of event A occurring given that event B is enforced. Unlike in CBNs, interventions in PCF are more general and do not require unique value assignments to manipulated random variables. Instead, the impact of an intervention depends on the critical set, allowing for different values for the same random variables in various branches of the tree. Moreover, it can manipulate different random variables in each branch, functioning as a context-dependent "recipe" to achieve the desired outcome.

MIMIC-IV: To elucidate the impact of key physiological parameters on ICU length of stay (LOS), an interventional anal-

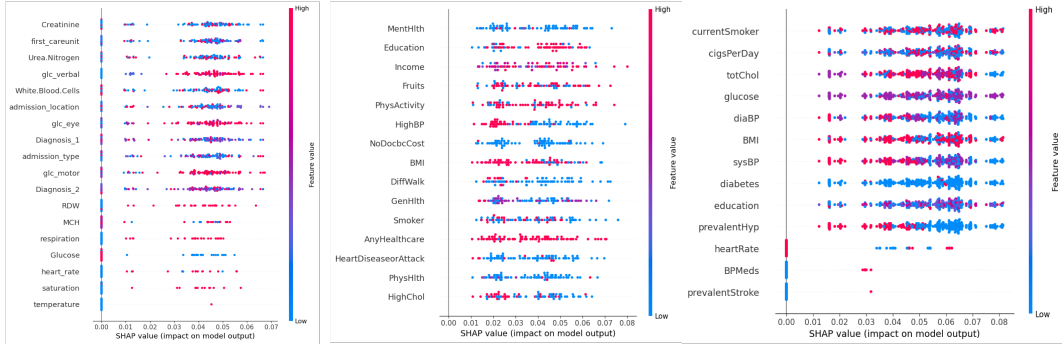


Figure 3: SHAP plot showing feature impacts on predictions for LOS, CHD, and Diabetes.

ysis was conducted. Eight critical factors were examined to assess the PCF model’s ability to replicate established causal relationships. The primary objective was to assess PCFs ability to replicate established causal relationships between these parameters and LOS. Box plots (Figure 4) were used to visualise the distribution of los across different intervention groups. In these plots, red signifies an increased probability of los exceeding 4 days ($los = 1$), while green signifies a decrease.

Existing literature establishes a link between bradycardia (heart rate ≤ 60 beats per minute) and extended ICU stays due to underlying medical conditions requiring further investigation or treatment [58]. To explore this relationship within our model, interventional analysis was conducted on heart rate. Simulating bradycardia ($do(heart_rate = 0)$) significantly increased the likelihood of extended ICU stays ($los = 1$), consistent with established medical knowledge. However, the relationship between heart rate and length of stay is more complex. Similar trends were observed for heart rates above 60 bpm ($do(heart_rate = 1)$), though to a lesser extent, and a slight decrease in $los = 1$ was noted for even higher heart rates ($do(heart_rate = 2)$). This highlights the need to consider multiple physiological and clinical variables beyond heart rate.

In literature, it is established that low levels of urea nitrogen (UN) are not typically concerning, often associated with low protein intake [59]. Similar findings are observed in our model, where manipulating UN levels to be low ($do(Urea_Nitrogen = 0)$) results in a decrease in the proportion of patients with extended ICU stays ($los = 1$). However, as the intervention values increase ($do(Urea_Nitrogen = 1)$ and $do(Urea_Nitrogen = 2)$), a trend emerges indicating a potential rise in the probability of $los = 1$. While this increase is subtle, it is visually detectable by the red color in the box plots.

Literature indicates that elevated Red Cell Distribution Width (RDW) is closely associated with increased risk of cardiovascular morbidity and mortality in patients with previous myocardial infarction, potentially leading to prolonged hospital stays [60]. Our model’s interventional analysis, where RDW is manipulated to be high ($do(RDW = 2)$), shows a corresponding increase in the percentage of patients with extended ICU stays ($los = 1$), consistent with existing literature.

Lower levels of creatinine are often related to muscle loss and severe liver disease. Patients experiencing significant mus-

cle mass loss in the first week of ICU admission are at higher risk of extended stays [61]. This aligns with our findings, where intervening to set low creatinine levels ($do(Creatinine = 0)$) notably increases the likelihood of extended ICU stays ($los = 1$).

High respiration rate, indicative of tachypnea in adults, is characterised by a respiratory rate exceeding 20 breaths per minute and often requires further assessment, leading to prolonged hospital stays [62]. In our model, intervening to elevate the respiration rate ($do(respiration = 2)$) resulted in an increased probability of extended ICU stays ($los = 1$).

Fever is a common issue in ICU patients and often necessitates diagnostic tests and procedures, which significantly prolongs the stay [63]. Consistent with this, our model shows that intervening to indicate mild fever ($do(temperature = 1)$) also leads to an elevated probability of extended ICU stays ($los = 1$).

Inadequate oxygen saturation ($do(saturation = 1)$) has a varied effect on $los = 1$, while other saturation levels show no discernible impact. Manipulating glucose levels reveals an inverse response, suggesting these variables indirectly influence LOS through intermediary factors rather than exerting a direct effect.

Framingham Heart Data: This section explores the impact of various health factors on CHD risk through intervention analysis, aiming to assess the PCF’s ability to replicate established causal relationships between these parameters and CHD. As illustrated in 5, our findings underscore significant alterations in $P(TenYearCHD = 1)$ across different interventions, shedding light on the intricate interplay between these health factors and CHD risk.

Existing literature highlights both systolic and diastolic hypertension as independent risk factors for adverse cardiovascular events [64]. Our analysis corroborates this, demonstrating that interventions on systolic blood pressure, such as $do(sysBP = 3)$, result in an increased probability of $CHD = 1$. Similarly, interventions on diastolic blood pressure ($do(diaBP = 1)$, $do(diaBP = 2)$ and $do(diaBP = 3)$) also heighten the likelihood of $CHD = 1$, reinforcing the significant impact of blood pressure levels on cardiovascular health.

Additionally, glucose metabolism plays a critical role in cardiovascular health, as deviations from normal glucose levels can lead to adverse outcomes [65]. Our model confirms this relationship, showing that interventions altering glucose levels, such as $do(glucose = 0)$ and $do(glucose = 2)$, significantly in-

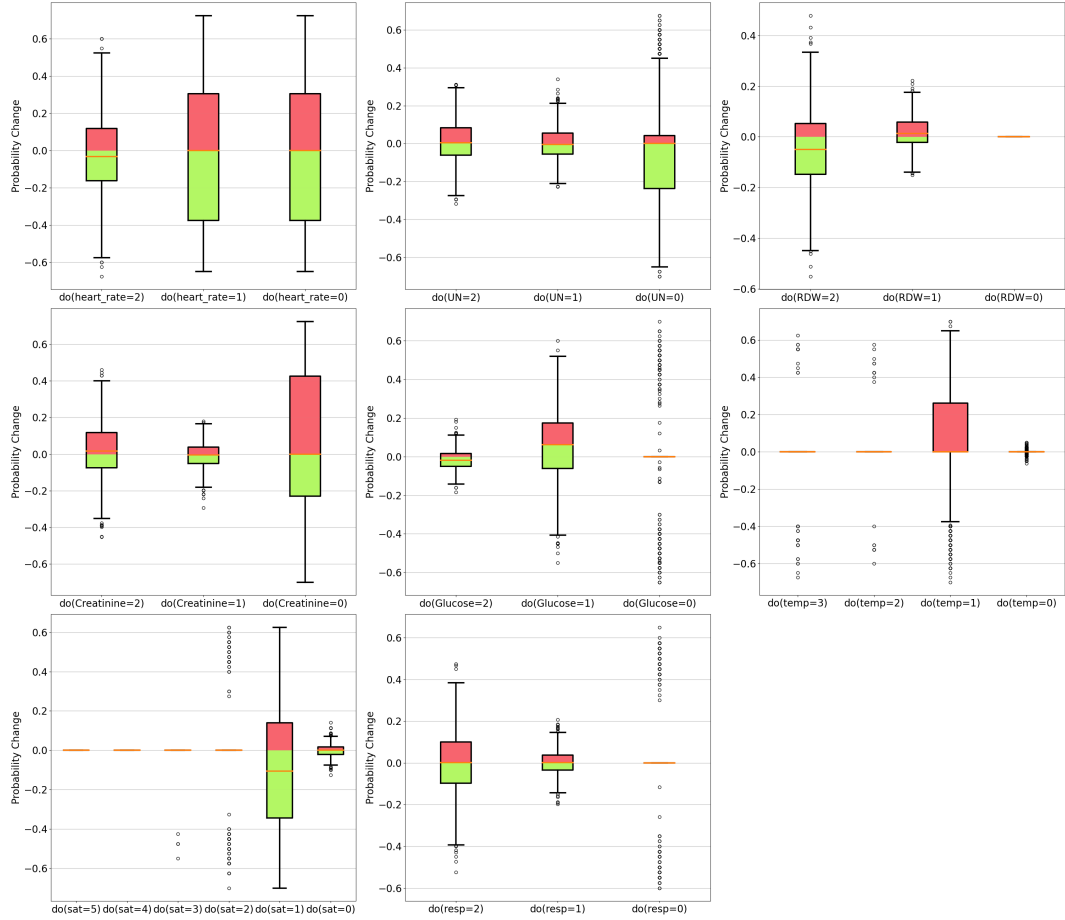


Figure 4: Probability change of los given interventions on heart_rate, Urea_Nitrogen (UN), RDW, Creatinine, Glucose, temperature (temp), saturation (sat), and respiration rate (resp)

crease the probability of $CHD = 1$. These findings underscore the critical role that glucose regulation plays in cardiovascular risk management.

Raised total cholesterol levels are well-documented as a significant risk factor for coronary heart disease (CHD) [66]. In our model, interventions on total cholesterol ($do(totChol = 1)$ i.e levels ≥ 200) were found to increase the probability of $CHD = 1$, reinforcing the established link between elevated cholesterol and heightened CHD risk.

Literature highlights that asymptomatic bradycardia may influence heart disease risk due to underlying autonomic or cardiovascular issues [67]. Our intervention analysis, which simulates bradycardia through interventions on heart rate ($do(heartRate = 0)$), reveals a marked increase in the probability of $CHD = 1$.

Smoking has been highlighted as a leading risk factor for heart disease [68]. Our model's interventions demonstrate that smoking 6-10 cigarettes per day ($do(cigsPerDay = 2)$) and more than 11 cigarettes per day ($do(cigsPerDay = 3)$) significantly increase the probability of $CHD = 1$. These findings underscore the substantial impact of smoking on coronary heart disease risk.

Research indicates that higher education levels can lead to substantial health benefits [69]. Our model corroborates these

findings, demonstrating that higher levels of education significantly decrease the probability of $CHD = 1$.

The relationship between BMI and CHD is often characterised as inconsistent and complex [70]. Our findings support this observation, as BMI interventions did not produce interpretable results. This ambiguity may be attributed to the intricate interplay of metabolic factors that extend beyond body mass alone, suggesting that BMI might not be a straightforward predictor of CHD risk. The lack of a clear relationship underscores the need for a more nuanced understanding of how metabolic factors contribute to CHD.

Diabetes: This section explores the influence of various health factors on the likelihood of developing diabetes through intervention analysis. As depicted in Figure 6, illustrates the significant changes in diabetes risk ($P(Diabetes = 1)$) following interventions on the selected variables.

Hypertension and hyperlipidemia are well-established predictors of diabetes risk, as highlighted in existing literature [71, 72]. Our analysis confirms this relationship, showing that high blood pressure ($do(HighBP = 1)$) increases diabetes probability, while its absence ($do(HighBP = 0)$) decreases the risk. Similarly, elevated cholesterol levels ($do(HighChol = 1)$) are linked to a higher likelihood of diabetes, whereas normal

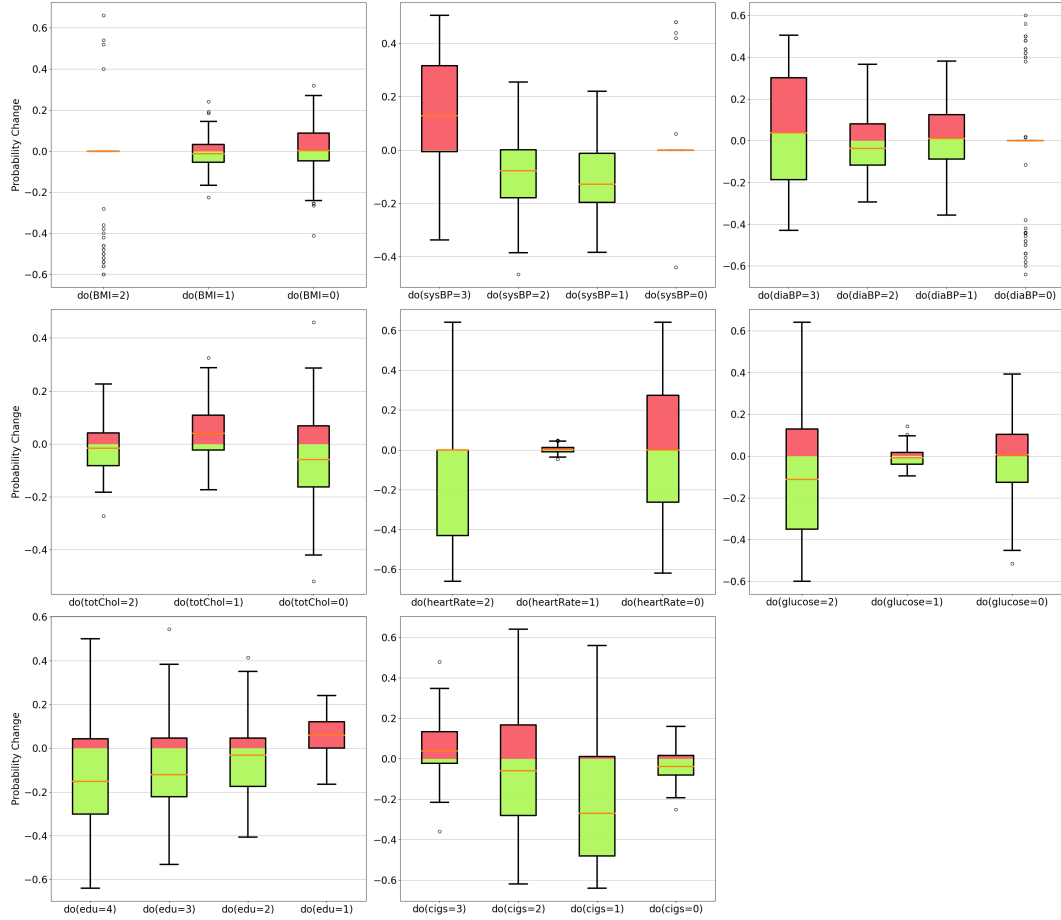


Figure 5: Probability change of TenYearCHD given interventions on sysBP, diaBP, totChol, BMI, education, glucose, heartRate and cigsPerDay.

cholesterol levels ($do(HighChol = 0)$) reduce the risk.

Body Mass Index (BMI) is another significant risk factor for diabetes [73]. Our findings indicate that maintaining a normal BMI ($do(BMI = 0)$) lowers the probability of diabetes, while a BMI of 40 or more ($do(BMI = 2)$) substantially raises this probability. This suggests that keeping a BMI between 0-24 mitigates diabetes risk, whereas higher BMI levels considerably elevate it.

Maintaining a healthy lifestyle is crucial for diabetes prevention [74]. Our analysis demonstrates that individuals with excellent general health ($do(GenHlth = 1)$) have a lower risk of developing diabetes compared to those in good ($do(GenHlth = 2)$) or poor health ($do(GenHlth = 3)$). Additionally, regular physical activity ($do(PhysActivity = 1)$) significantly reduces diabetes risk compared to a sedentary lifestyle ($do(PhysActivity = 0)$).

Education also plays a positive role in diabetes management and complication prevention [75]. Our results indicate that individuals with limited education ($do(education = 1)$) face a higher diabetes risk, while those with some secondary education ($do(education = 2)$) show mixed outcomes. Notably, higher education levels ($do(education = 3)$) are significantly associated with reduced diabetes risk.

The link between diabetes and heart disease is well-

documented [76]. Our analysis supports this connection, as the absence of heart disease ($do(HeartDisease = 0)$) decreases diabetes risk, whereas its presence ($do(HeartDisease = 1)$) significantly increases it. This finding underscores the interconnected nature of these conditions, highlighting the need for integrated healthcare strategies.

5.4. Counterfactuals

Counterfactuals are alternative scenarios or outcomes that could have occurred if certain events or variables had been different. In healthcare, they can be used to explore what would have happened if a different course of action was taken or if certain variables were changed. Counterfactual statements enable clinicians to investigate the probabilities associated with an 'alternate reality'. They distinguish between the indicative, which is the factual situation (events that have actually happened), and the subjunctive (events that could have occurred in an alternate reality). In this study we investigated two distinct counterfactual scenarios to assess the impact of clinician insights on our model which have been explained in Section 5.4.1 and 5.4.2.

5.4.1. Reordering Variables Based on Domain Knowledge

We investigate the impact of modifying variable order within the PCF framework to illustrate its potential benefits as a proof

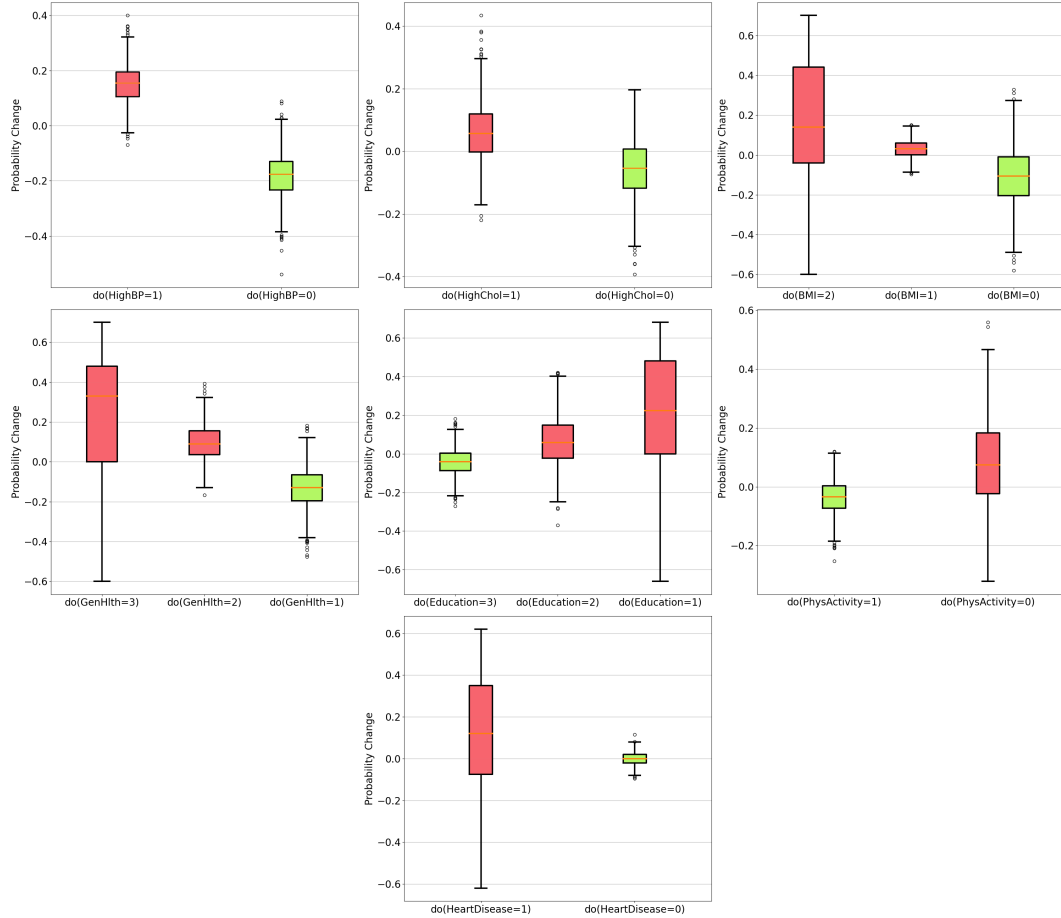


Figure 6: Probability change of Diabetes given interventions on sysBP, diaBP, totChol, BMI, education, glucose, heartRate and cigsPerDay.

of concept, rather than an implementation of clinician-directed decisions. While the CBN provides a robust foundational structure, our intent is to demonstrate how the model could be enhanced by integrating clinician-informed causal relationships. The core principle of our model is adaptability; it combines empirical foundations provided by the CBN with potential clinical insights. While the CBN’s causal structure establishes the initial framework, we explore how clinician adjustments to the variable order might impact predictive precision.

By granting clinicians the ability to adjust variable sequences, we create an inclusive environment where domain-specific knowledge can shape and refine the model’s architecture. This approach aims to balance the structured scaffolding provided by the CBN with the nuanced insights derived from clinical acumen, ultimately enriching the model’s interpretability and operational efficacy in real-world healthcare settings. This fosters the exploration of counterfactual scenarios, assessing the impact of incorporating clinician insights on model performance and decision-making outcomes.

Soliciting specific feedback on variables, assumptions, and potential causal relationships enhances the interpretability, relevance, and trustworthiness of our model, ensuring alignment with clinical expertise and practice. Through this refinement, we navigate diverse scenarios or “what-if” queries related to the

model’s operation under distinct conditions, including modifications of causal trajectories informed by clinical expertise.

Figure 7 illustrates the process by which large hospitals, equipped with extensive datasets, can develop CBNs to represent causal relationships. These hospitals can then create pre-trained PCF models. These models can be securely shared with smaller hospitals, facilitating efficient knowledge transfer and collaborative decision-making in healthcare. The figure also demonstrates how re-ordering variables provides feedback to the Centralised CBN, showcasing the integration of clinical insights into the model’s development.

MIMIC-IV. The initial variable order provided by the CBN positioned “Diagnosis_2” earlier in the sequence, suggesting its early influence on the outcome variable. However, the counterfactual adjustment hypothesised that strategically reordering the variables might enhance the model’s capacity to learn causal relationships and predict *los* more accurately. This adjustment reflected the potential causal flow where “Diagnosis_2” is informed by preceding laboratory tests. Therefore, we reordered the variables to place “Diagnosis_2” later in the sequence, just before the outcome variable (*los*).

Table 4 summarises the performance of the PCF and PTree methods following the variable order change. The table reveals that while the rearrangement did not alter the accuracy of the

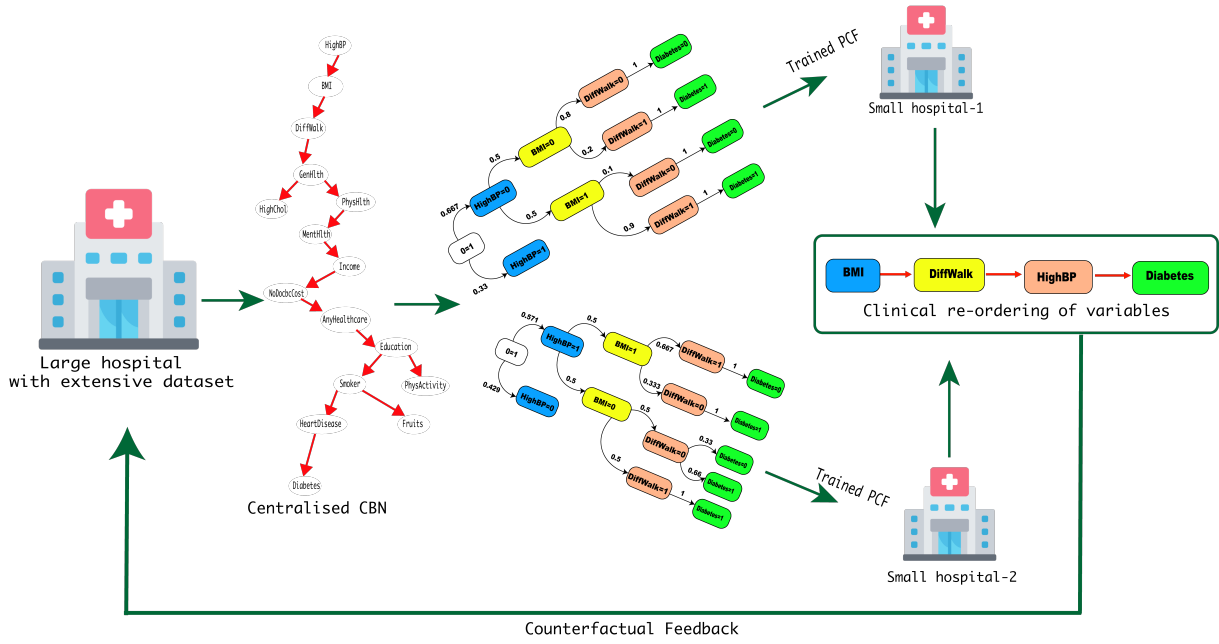


Figure 7: The process of developing and sharing pre-trained PCFs by large hospitals with extensive datasets. The feedback loop illustrates how re-ordering variables integrates clinical insights into the Centralised CBN, enhancing collaborative decision-making in healthcare.

Table 4

Results using SMOTE for MIMIC-IV after changing the order

Algorithm	Accuracy	Specificity	Sensitivity	AUC-ROC
Ptree	80.29	91.11	40.06	65.59
PCF	72.43	78.33	50.50	64.41

Table 5

Results using SMOTE for framingham data after changing the order

Algorithm	Accuracy	Specificity	Sensitivity	AUC-ROC
Ptree	64.98	69.40	40.31	54.85
PCF	66.39	69.12	51.16	60.14

Table 6

Results using ADASYN for diabetes data after changing the order

Algorithm	Accuracy	Specificity	Sensitivity	AUC-ROC
Ptree	73.29	78.93	38.14	58.54
PCF	73.71	75.45	62.88	69.17

Ptree model, it resulted in a slight decrease in PCF performance. This outcome might be attributed to the sensitivity of the PCF model to variable order, as it relies on an intricate interplay of causality among variables. The reordering may have disrupted previously established dependencies, highlighting the complex interactions inherent in the data. Such changes underline the importance of carefully considering the sequence of variables in models sensitive to causal relationships.

Framingham Heart Data: The original variable order provided by the CBN included 'BPMeds', 'prevalentHyp', 'heartRate', 'prevalentStroke', 'diabetes', 'sysBP', 'totChol', 'glucose', 'diaBP', 'BMI', 'education', 'currentSmoker', 'cigsPerDay', and 'TenYearCHD'. Subsequently, a counterfactual adjustment was made, rearranging certain variables to create a revised order: 'BPMeds', 'prevalentHyp', 'diabetes', 'glucose', 'heartRate', 'sysBP', 'diaBP', 'BMI', 'education', 'totChol', 'prevalentStroke', 'currentSmoker', 'cigsPerDay', and 'TenYearCHD'

Table 5 presents the performance evaluation results for the PCF and Ptree methods following the variable order modification. The analysis indicates almost similar performance for both the PCF and Ptree method (slightly lower than original). This slight decrease can be attributed to the fact that the original order might have implicitly captured relevant relationships for

CHD prediction better than the counterfactual order.

Diabetes: The original order of variables provided by the CBN was as follows: 'HighBP', 'BMI', 'DiffWalk', 'GenHlth', 'PhysHlth', 'HighChol', 'MentHlth', 'Income', 'NoDocbcCost', 'AnyHealthcare', 'Education', 'Smoker', 'PhysActivity', 'HeartDiseaseorAttack', 'Fruits', 'Diabetes.binary'. The counterfactual order maintained the overall structure but changed the position of a few variables and the new order became: 'GenHlth', 'BMI', 'DiffWalk', 'PhysHlth', 'PhysActivity', 'HighBP', 'HighChol', 'MentHlth', 'Education', 'Income', 'NoDocbcCost', 'AnyHealthcare', 'Smoker', 'HeartDiseaseorAttack', 'Fruits', 'Diabetes.binary'.

Table 6 summarises the accuracy of PCF and Ptree methods, after the change in variable order. As the table shows, reordering the variables led to an increase in the model accuracy for PCF as well as for Ptree. However, AUC-ROC seems to have decreased in both.

5.4.2. Counterfactual Statements for Specific Datasets

Counterfactual analysis within PCF allows the exploration of different paths a stochastic process might have taken. It examines "what-if" scenarios where specific variables take on different values than in reality. This technique evaluates conditional probabilities of the form $P(A_C | B)$, representing the probability of event A occurring under the counterfactual assumption that event C is true, given that event B is factual (observed). Here, A_C denotes the subjunctive event A under the counterfactual assumption that the event C has occurred (i.e. a potential response), and B is the indicative (i.e. factual) assumption. A counterfactual PCF is constructed by modifying a reference model through factual statements, and then spawning a new variable scope from a counterfactual modification, formalised as an intervention. The intervention effectively resets the state of downstream variables by replacing their existing values with their initial unbound state. The computation of counterfactuals can be achieved algorithmically, as outlined in [8]. While the power of counterfactual explanations lies in their ability to explore alternative realities, computational tractability and interpretability necessitate a focus on feature sparsity. In simpler terms, it is more computationally efficient and interpretable to manipulate a limited number of key features within the model. This prioritises generating actionable insights by focusing on interventions that are realistic and have the potential to be implemented in practice. The burgeoning field of counterfactual explainability [77] emphasises the critical importance of imposing constraints on the types of interventions considered. These constraints ensure that counterfactual explanations are not only theoretically robust but also practically applicable in real-world decision-making contexts. Guided by this principle, we carefully selected features for each dataset that offer the most valuable insights into how targeted interventions can influence predicted outcomes. This selection process was heavily informed by their established presence and significance in the existing literature. Incorporating well-researched variables enhances the relevance and reliability of our counterfactual analyses, ultimately improving the practical utility of our findings. Figure 8 presents a visual representation of counterfactual analysis.

MIMIC-IV: This section explores the factors influencing the LOS in the ICU using counterfactual analysis. Specifically, we examine the conditional probability of a patient requiring an extended ICU stay ($los = 1$, i.e., more than 4 days). By employing counterfactual explanations, we investigate hypothetical scenarios where certain vital signs or laboratory values are altered. This allows us to assess the impact of these changes on the probability of an extended ICU stay. Features were chosen based on their potential to yield valuable insights into the determinants of prolonged ICU stays.

- a) **Heart Rate:** We analysed the effect of heart rate by comparing the baseline probability ($P(los = 1|heart_rate = 0)$) for patients with low heart rate (0) to the counterfactual scenario where their heart rate is normal (1). The counterfactual probability ($P(los^* = 1|heart_rate = 0), los^* =$

$los[heart_rate < -1]$) suggests a decrease in the likelihood of extended ICU stay when the heart rate is normal.

- b) **Saturation:** Similarly, we examined the effect of oxygen saturation by comparing baseline probability of ($P(los = 1|saturation = 3)$) for patients with very low oxygen saturation (3) to the counterfactual scenario with normal oxygen saturation (0). The counterfactual probability ($P(los^* = 1|saturation = 3), los^* = los[saturation < -0]$) indicates that there is a marginal difference in the probability of an extended ICU stay when the patient's saturation level is normal.
- c) **Glucose and Urea Nitrogen:** We further analysed the role of glucose and Urea Nitrogen levels. Interestingly, for both high glucose ($P(los = 1|Glucose = 2)$) and high Urea Nitrogen ($P(los = 1|UreaNitrogen = 2)$), the counterfactual scenarios with normal levels (glucose = 1 and Urea Nitrogen = 1, respectively) showed slightly increased probabilities of extended ICU stay ($P(los^* = 1|Glucose = 2), los^* = los[Glucose < -1]$ and $P(los^* = 1|UreaNitrogen = 2), los^* = los[UreaNitrogen < -1]$). Thus, the probability of extended ICU stay may be increased even if the patient had normal glucose and urea nitrogen levels.
- d) **Temperature:** Finally, we explored the influence of body temperature. The baseline probability for extended ICU stay with high fever ($P(los = 1|temperature = 2)$) was compared to the counterfactual scenario with normal temperature (0). This resulted in a minor decrease in the probability ($P(los^* = 1|temperature = 2), los^* = los[temperature < -0]$) which suggests a slight decrease in the likelihood of extended ICU stay, if the patient had normal body temperature.

Figure 9 illustrates the probability of a patient remaining in the ICU for more than four days ($los = 1$) under various counterfactual scenarios involving five different variables: Heart Rate, Saturation, Glucose, Urea, and Temperature. Each line in the plot represents one of these variables, with the x-axis displaying the factual and counterfactual scenarios and the y-axis showing the probability values. This figure provides insights into how alterations in these variables influence the likelihood of an extended ICU stay.

Framingham Data: This data offers a wealth of information on cardiovascular risk factors. To leverage counterfactual explanations effectively, we strategically select the features with high explanatory potential for predicting CHD.

- a) **BMI:** We began our analysis by examining the impact of Body Mass Index (BMI) on the likelihood of developing CHD. Starting with a BMI of 2 (High), indicative of CHD, we delved into counterfactual scenarios to explore the probability of CHD had the patient possessed a normal BMI (0). The baseline probability $P(CHD = 1|BMI = 2)$ represents the likelihood of CHD under the existing BMI condition. Interestingly, the counterfactual probability

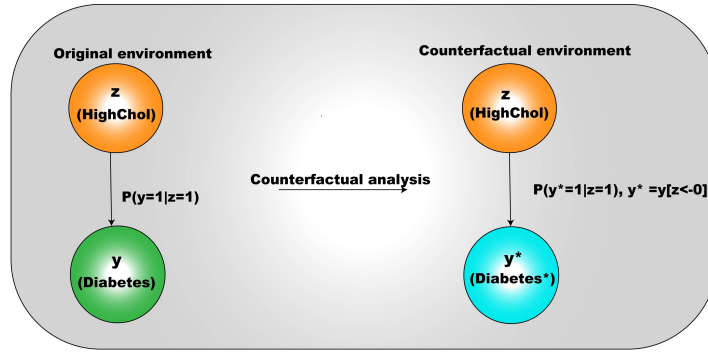


Figure 8: Visualisation of Counterfactual statements

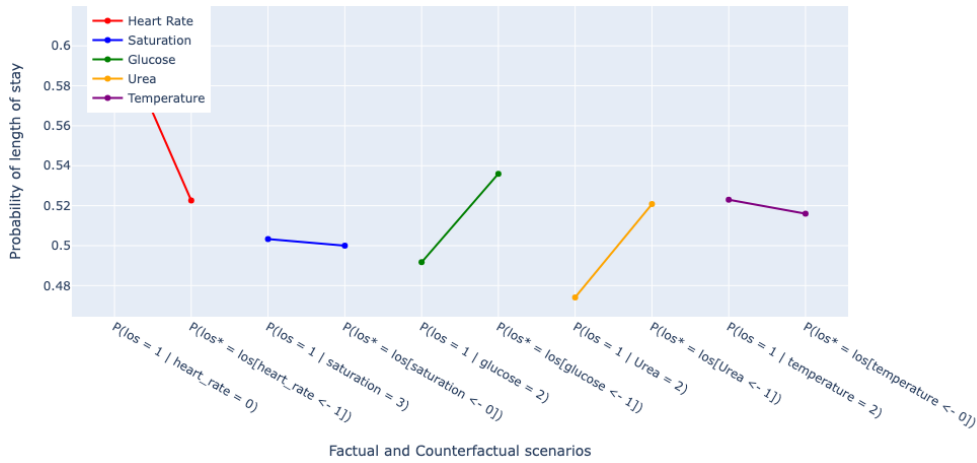


Figure 9: Line plots showing the probability of ICU stay exceeding 4 days under factual and counterfactual scenarios for various health variables.

$P(\text{CHD}^* = 1 | \text{BMI} = 2)$, $\text{CHD}^* = \text{CHD}[\text{BMI} < -0]$ reveals that even with a normal BMI, the risk of CHD might still remain relatively high.

- b) **Systolic Blood Pressure (sysBP) and Diastolic Blood Pressure (diaBP):** We investigated the influence of blood pressure measurements (systolic pressure, or sysBP, and diastolic pressure, or diaBP) of patients on CHD prevalence. Individuals with high blood pressure (represented by a score of 3 for both sysBP and diaBP) were found to have a higher chance of having CHD ($P(\text{CHD} = 1 | \text{sysBP} = 3)$ and $P(\text{CHD} = 1 | \text{diaBP} = 3)$). We then considered a hypothetical scenario: what if these patients with high blood pressure had normal values instead (sysBP = 1 and diaBP = 1)? The corresponding probabilities, ($P(\text{CHD}^* = 1 | \text{sysBP} = 3)$, $\text{CHD}^* = \text{CHD}[\text{sysBP} < -1]$ and $P(\text{CHD}^* = 1 | \text{diaBP} = 3)$, $\text{CHD}^* = \text{CHD}[\text{diaBP} < -1]$), show how lowering blood pressure could potentially decrease the risk of CHD.
- c) **Total Cholesterol (totChol):** We explored the potential influence of total cholesterol (totChol) on the development

of CHD using counterfactual analysis. In the factual scenario, we assessed patients based on their actual totChol (totChol = 3). The baseline probability was determined as $P(\text{CHD} = 1 | \text{totChol} = 3)$. In the counterfactual scenario, we posed the question: what if these patients with high totChol had normal values (totChol = 0)? The resulting probability $P(\text{CHD}^* = 1 | \text{totChol} = 3)$, $\text{CHD}^* = \text{CHD}[\text{totChol} < -0]$ suggests that maintaining normal total cholesterol levels might be beneficial for reducing CHD risk.

- d) **Cigarettes per day (cigsPerDay):** Finally, we explored the influence of smoking. In the factual scenario, we examined patients based on their actual cigarette consumption (cigsPerDay = 3). The baseline probability was determined as $P(\text{CHD} = 1 | \text{cigsPerDay} = 3)$. The counterfactual scenario asks, "what if" these patients who smoke heavily cigsPerDay = 3 (≥ 11 cigarettes/day) had never smoked (cigsPerDay = 0)? The resulting probability $P(\text{CHD}^* = 1 | \text{cigsPerDay} = 3)$, $\text{CHD}^* = \text{CHD}[\text{cigsPerDay} < -0]$ suggests that quitting smoking could be beneficial for reducing CHD risk.

Figure 10 illustrates the line plots generated to explore the distribution of risk factors for CHD using counterfactual analysis. It can be observed that the counterfactual scenarios pertaining to sysBP, diaBP, totChol and cigsPerDay potentially change the probability of $CHD = 1$.

Diabetes Data: This section explores the application of counterfactual explanations within the diabetes dataset. By strategically selecting features, we focus on identifying modifiable risk factors.

- a) **HighBP:** We examined the relationship between HighBP and the prevalence of diabetes. In the actual scenario, patients were evaluated based on their recorded blood pressure levels (HighBP = 1). The baseline probability was calculated as $P(Diabetes.binary = 1|HighBP = 1)$. However, in the hypothetical scenario, we posed the question: what if these patients with high blood pressure had normal blood pressure (HighBP = 0)? The resulting probability $P(Diabetes.binary^* = 1|HighBP = 1), Diabetes.binary^* = Diabetes.binary[HighBP < -0]$, suggests a potential benefit of maintaining normal blood pressure to reduce the risk of diabetes. This is in accordance to the literature which states that Blood pressure control is just as important as glycemc control [78].
- b) **HighChol:** We examined the influence of high cholesterol (HighChol) on the prevalence of Diabetes. In the factual scenario, patients were evaluated based on their actual cholesterol measurements (HighChol = 1). The baseline probability was computed as $P(Diabetes.binary = 1|HighChol = 1)$. However, in the counterfactual scenario, we considered: what if these patients with high cholesterol had normal levels (HighChol = 0)? The resulting probability $P(Diabetes.binary^* = 1|HighChol = 1), Diabetes.binary^* = Diabetes.binary[HighChol < -0]$ highlights the potential advantage of normalising cholesterol levels in mitigating the risk of diabetes.
- c) **BMI:** We explored the impact of BMI on diabetes prevalence using counterfactual analysis. In the factual scenario, we assessed patients based on their actual BMI (BMI = 2). The baseline probability was $P(Diabetes.binary = 1|BMI = 2)$. The counterfactual scenario investigated the hypothetical scenario where patients with high BMI (BMI = 2) had a normal BMI (BMI = 0). We aimed to determine the impact of this hypothetical change on diabetes risk. The resulting probability, $(P(Diabetes.binary^* = 1|BMI = 1), Diabetes.binary^* = Diabetes.binary[BMI < -0])$, suggests a potential benefit of maintaining a healthy weight (represented by normal BMI) in reducing diabetes risk.
- d) **GenHealth:** This study investigated the link between a patient’s overall health (GenHealth) and their risk of developing diabetes using counterfactual analysis. The indicative premise is that the patient has poor health (GenHealth =3), and the subjunctive (counterfactual) premise is if the patient has excellent health

(GenHealth =1) in an alternate reality. The baseline probability was determined as $P(Diabetes.binary = 1|GenHealth = 3)$. The probability resulting from the subjunctive premise, $P(Diabetes.binary^* = 1|GenHealth = 3), Diabetes.binary^* = Diabetes.binary[GenHealth < -1]$ illustrates the potential benefit of maintaining the overall well-being so as to reduce the risk of diabetes.

Figure 11 illustrates the change in $P(Diabetes = 1)$ as a result of the counterfactual statements described.

6. Conclusion

This study introduces the Probabilistic Causal Fusion (PCF) framework, which combines Causal Bayesian Networks (CBNs) and Probability Trees (PTrees) to enhance healthcare decision-making. This innovative approach harnesses the causal structure learned by the CBN to establish the foundational framework of the PTree. This synergy yields a three-fold benefit: (1) it captures the inherent causal relationships within the data, leading to a more robust understanding of the factors influencing outcomes, (2) it facilitates the incorporation of domain knowledge through counterfactual analysis, empowering clinicians to integrate their expertise into the model, and (3) it facilitates the creation of a centralised repository of causal knowledge across institutions. This fosters collaboration, knowledge exchange, and continuous improvement in healthcare delivery.

Rigorous validation using three real-world medical datasets demonstrates that the proposed methodology achieves prediction performance on par with established models. However, its true strength lies in its ability to surpass mere prediction and empower clinicians. Unlike traditional machine learning methods, this framework facilitates the exploration of hypothetical interventions and counterfactual scenarios through counterfactual analysis.

This enhanced functionality translates into a more comprehensive toolkit for healthcare professionals. It enables them to not only predict patient outcomes with established accuracy but also to simulate the potential effects of treatment strategies and analyse the impact of alternative scenarios. This deeper understanding of risk factor interactions, intervention effects, and the flexibility to explore variable ordering significantly improves clinical decision-making, ultimately leading to optimised patient care.

A key strength of this approach is its dual applicability at the individual and population levels. Clinicians can leverage this framework to gain insights into broader population trends while simultaneously exploring personalised treatment options for specific patients through counterfactual analysis. This versatility empowers healthcare professionals to tailor their decision-making to the unique circumstances of each patient while simultaneously informing clinical best practices for the entire population.

Our study suggests that this approach holds significant promise for evidence-based clinical decision-making. However, further exploration is needed to address certain limita-

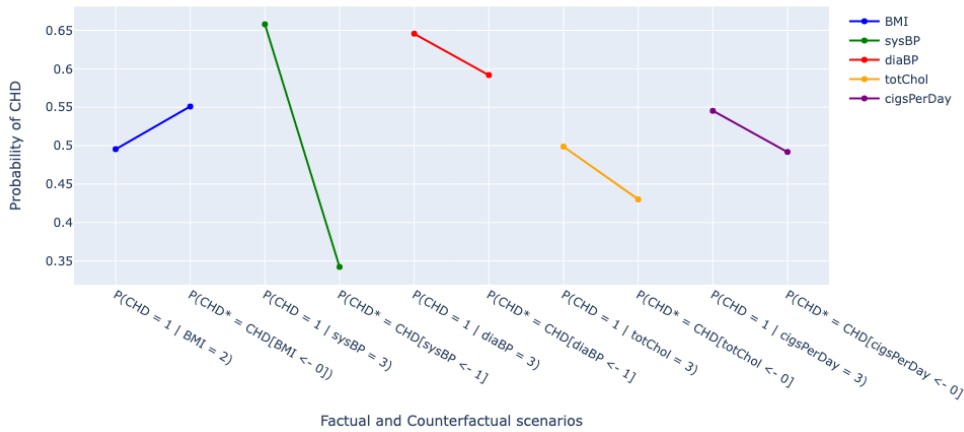


Figure 10: Probability distribution of TenYearCHD for factual and counterfactual scenarios for various variables.

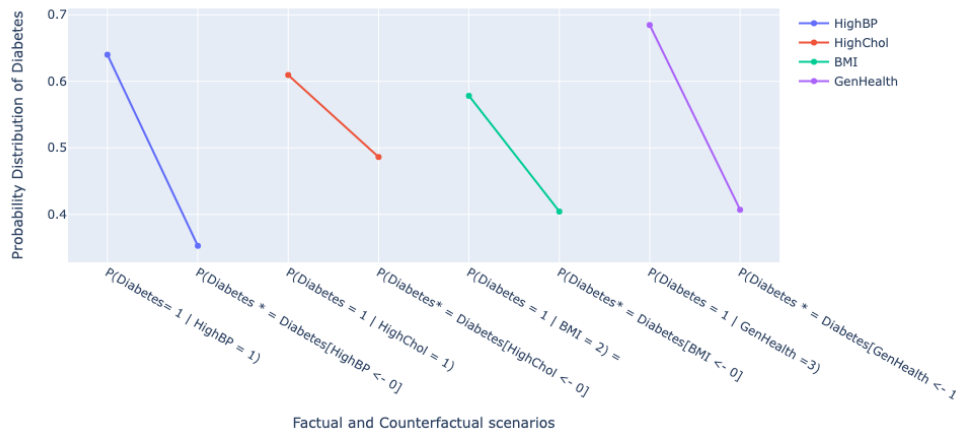


Figure 11: Probability Distribution of Diabetes for factual and counterfactual scenarios for various variables.

tions. Optimising computational efficiency, especially for large datasets, is crucial for broader applicability. While this study focused on specific medical domains, future research should investigate the framework’s generalisability to a wider range of healthcare settings. Incorporating clinical expertise in selecting variables for counterfactual and interventional analysis is essential. Clinicians’ insights can refine the methodology and enhance its practical utility by ensuring the system uses the most relevant and useful data.

Addressing these limitations and broadening the scope of applications, including genomic data analysis, will further demonstrate the framework’s potential to advance healthcare. Building on this approach can lead to the development of more effective and transparent tools that enhance patient care. Such tools have the potential to support evidence-based clinical decision-making and contribute to a more efficient and impactful healthcare system overall.

CRedit Authorship Contribution Statement

Sheresh Zahoor: Conceptualization, Methodology, Data curation, Visualization, Formal analysis, Investigation, Resources, Software, Validation, Writing – original draft, Writing – review and editing. **Pietro Liò:** Conceptualization, Investigation, Resources, Supervision, Validation, Writing – review and editing. **Gaël Dias:** Conceptualization, Supervision, Validation, Writing – review and editing. **Mohammed Hasanuz-zaman:** Conceptualization, Supervision, Validation, Writing – review and editing.

Declaration of Competing Interest

The authors declare that they have no known competing financial interests or personal relationships that could have appeared to influence the work reported in this paper.

Acknowledgments

This work has been jointly supported by Research Ireland [Grant number 18/CRT/6222] and the European Union’s Horizon 2020 research and innovation programme [Grant agreement number 101017385]. Additionally, for the purpose of Open Access, the author has applied a CC BY public copyright licence to any Author Accepted Manuscript version arising from this submission.

References

- [1] J. Pearl, *Causality: Models, Reasoning and Inference*, Cambridge University Press, (2009).
URL <http://bayes.cs.ucla.edu/B00K-2K/neuberg-review.pdf>
- [2] P. Sanchez, J. P. Voisey, T. Xia, H. I. Watson, A. Q. O’Neil, S. A. Tsaftaris, Causal machine learning for healthcare and precision medicine, *Royal Society Open Science* 9 (8) (2022) 220638. doi:<https://doi.org/10.1098/rsos.220638>.
URL <https://royalsocietypublishing.org/doi/10.1098/rsos.220638>
- [3] L. Kopitar, P. Kocbek, L. Cilar, A. Sheikh, G. Stiglic, Early detection of type 2 diabetes mellitus using machine learning-based prediction models, *Scientific reports* 10 (1) (2020) 11981.
- [4] S. Feuerriegel, D. Frauen, V. Melnychuk, J. Schweisthal, K. Hess, A. Curth, S. Bauer, N. Kilbertus, I. S. Kohane, M. van der Schaar, Causal machine learning for predicting treatment outcomes, *Nature Medicine* 30 (4) (2024) 958–968.
- [5] M. Prosperii, Y. Guo, M. Sperrin, J. S. Koopman, J. S. Min, X. He, S. Rich, M. Wang, I. E. Buchan, J. Bian, Causal inference and counterfactual prediction in machine learning for actionable healthcare, *Nature Machine Intelligence* 2 (7) (2020) 369–375. doi:<https://doi.org/10.1038/s42256-020-0197-y>.
URL <https://www.nature.com/articles/s42256-020-0197-y>
- [6] V. K. Rajput, M. K. Kalsoft, J. Dowie, The causal plausibility decision in healthcare, in: *pHealth 2022*, IOS Press, 2022, pp. 75–88. doi:[10.3233/SHTI220965](https://doi.org/10.3233/SHTI220965).
- [7] E. L. Ambags, G. Capitoli, V. L. Imperio, M. Provenzano, M. S. Nobile, P. Liò, Assisting clinical practice with fuzzy probabilistic decision trees (2023). arXiv:2304.07788, doi:<https://doi.org/10.48550/arXiv.2304.07788>.
- [8] T. Genewein, T. McGrath, G. Delétang, V. Mikulik, M. Martić, S. Legg, P. A. Ortega, Algorithms for causal reasoning in probability trees, arXiv preprint arXiv:2010.12237 (2020). doi:<https://doi.org/10.48550/arXiv.2010.12237>.
- [9] L. Chen, P. Ji, Y. Ma, Y. Rong, J. Ren, Custom machine learning algorithm for large-scale disease screening-taking heart disease data as an example, *Artificial Intelligence in Medicine* 146 (2023) 102688.
- [10] T. M. Usman, Y. K. Saheed, A. Nsang, A. Ajibesin, S. Rakshit, A systematic literature review of machine learning based risk prediction models for diabetic retinopathy progression, *Artificial intelligence in medicine* 143 (2023) 102617.
- [11] D. Mennicken, A. Rodríguez, M. Fariás-Jofré, J. Araya, E. Guzmán-Gutiérrez, Machine learning-based models for gestational diabetes mellitus prediction before 24–28 weeks of pregnancy: A review, *Artificial Intelligence in Medicine* 132 (2022) 102378.
- [12] M. M. Ahsan, Z. Siddique, Machine learning-based heart disease diagnosis: A systematic literature review, *Artificial Intelligence in Medicine* 128 (2022) 102289.
- [13] H. Ma, D. Li, J. Zhao, W. Li, J. Fu, C. Li, Hr-bcgn: Predicting readmission for heart failure from electronic health records, *Artificial Intelligence in Medicine* 150 (2024) 102829.
- [14] L. Yao, Z. Chu, S. Li, Y. Li, J. Gao, A. Zhang, A survey on causal inference, *ACM Transactions on Knowledge Discovery from Data (TKDD)* 15 (5) (2021) 1–46.
- [15] C. J. Blumberg, *Causal inference for statistics, social, and biomedical sciences: An introduction* (2016).
- [16] C. Belthangady, S. Giampanis, I. Jankovic, W. Stedden, P. Alves, S. Chong, C. Knott, B. Norgeot, Causal deep learning reveals the comparative effectiveness of antihyperglycemic treatments in poorly controlled diabetes, *Nature Communications* 13 (1) (2022) 6921.
- [17] J. G. Richens, C. M. Lee, S. Johri, Improving the accuracy of medical diagnosis with causal machine learning, *Nature communications* 11 (1) (2020) 3923.
- [18] P. W. Holland, Statistics and causal inference, *Journal of the American statistical Association* 81 (396) (1986) 945–960.
- [19] K. Rajendran, M. Jayabalan, V. Thiruchelvam, Predicting breast cancer via supervised machine learning methods on class imbalanced data, *International Journal of Advanced Computer Science and Applications* 11 (8) (2020).
- [20] P. Shahmirzalou, M. J. Khaledi, M. Khayamzadeh, A. Rasekhi, Survival analysis of recurrent breast cancer patients using mix bayesian network, *Heliyon* 9 (10) (2023).
- [21] B.-S. Jang, S.-J. Chun, H. S. Choi, J. H. Chang, K. H. Shin, et al., Estimating the risk and benefit of radiation therapy in (y) pN1 stage breast cancer patients: A bayesian network model incorporating expert knowledge (krog 22–13), *Computer Methods and Programs in Biomedicine* 245 (2024) pp. 108049.
- [22] J. M. Ordovás, D. Rios-Insua, A. Santos-Lozano, A. Lucia, A. Torres, A. Kosgodagan, J. M. Camacho, A bayesian network model for predicting cardiovascular risk, *Computer methods and programs in biomedicine* 231 (2023) pp. 107405. doi:[10.1016/j.cmpb.2023.107405](https://doi.org/10.1016/j.cmpb.2023.107405).
- [23] I. J. Dahabreh, K. Bibbins-Domingo, Causal inference about the effects of interventions from observational studies in medical journals, *JAMA* (2024).
- [24] A. Constantinou, The Bayesys user manual, <http://bayesianai.eecs.qmul.ac.uk/bayesys/>, [Online] Accessed 21 April 2023 (2019).
- [25] D. Heckerman, D. Geiger, D. M. Chickering, Learning bayesian networks: The combination of knowledge and statistical data, *Machine learning* 20 (1995) 197–243. doi:<https://doi.org/10.1023/A:1022623210503>.
- [26] R. R. Bouckaert, Properties of bayesian belief network learning algorithms, in: *Proceedings of the Tenth International Conference on Uncertainty in Artificial Intelligence*, Morgan Kaufmann Publishers Inc., San Francisco, CA, USA, 1994, p. 102–109. doi:<https://doi.org/10.1016/B978-1-55860-332-5.50018-3>.
- [27] R. Bouckaert, *Bayesian belief networks: from construction to inference*, Ph.D. thesis, University of Utrecht, Utrecht, Netherlands (1995).
URL <https://core.ac.uk/download/pdf/39700264.pdf>
- [28] A. C. Constantinou, Learning bayesian networks that enable full propagation of evidence, *IEEE Access* Vol. 8 (2020) pp. 124845–124856. doi:[10.1109/ACCESS.2020.3006472](https://doi.org/10.1109/ACCESS.2020.3006472).
URL <https://ieeexplore.ieee.org/document/9136714>
- [29] A. C. Constantinou, Y. Liu, N. K. Kitson, K. Chobtham, Z. Guo, Effective and efficient structure learning with pruning and model averaging strategies, *Int. J. Approx. Reasoning* Vol. 151 (C) (2022) pp. 292–321. doi:<https://doi.org/10.1016/j.ijar.2022.09.016>.
- [30] D. M. Chickering, C. Meek, Finding optimal bayesian networks, in: *Proceedings of the Eighteenth Conference on Uncertainty in Artificial Intelligence, UAI’02*, Morgan Kaufmann Publishers Inc., San Francisco, CA, USA, 2002, p. 94–102.
- [31] A. C. Constantinou, Z. Guo, N. K. Kitson, The impact of prior knowledge on causal structure learning, *Knowledge and Information Systems* 65 (8) (2023) 3385–3434. doi:<https://doi.org/10.1007/s10115-023-01858-x>.
URL <https://link.springer.com/article/10.1007/s10115-023-01858-x>
- [32] U. Kjærulff, L. C. Van Der Gaag, Making sensitivity analysis computationally efficient, arXiv preprint arXiv:1301.3868 (2013).
- [33] BayesFusion, GeNIe Modeler USER MANUAL, <https://support.bayesfusion.com/docs/GeNIe.pdf>, [Online] Accessed 21 April 2023 (2023).
- [34] P. Biecek, T. Burzykowski, *Explanatory model analysis: explore, explain, and examine predictive models*, Chapman and Hall/CRC, 2021.
- [35] J. C. Marshall, L. Bosco, N. K. Adhikari, B. Connolly, J. V. Diaz, T. Dorman, R. A. Fowler, G. Meyfroidt, S. Nakagawa, P. Pelosi, et al., What is an intensive care unit? a report of the task force of the world federation of societies of intensive and critical care medicine, *Journal of critical care*

- 37 (2017) 270–276. doi:10.1016/j.jcrr.2016.07.015.
- [36] M. H. Weil, W. Tang, From intensive care to critical care medicine: a historical perspective, *American journal of respiratory and critical care medicine* 183 (11) (2011) 1451–1453. doi:10.1164/rccm.201008-1341OE.
- [37] G. H. Robinson, L. E. Davis, R. P. Leifer, Prediction of hospital length of stay, *Health services research* 1 (3) (1966) 287.
- [38] K. Stone, R. Zwiggelaar, P. Jones, N. Mac Parthaláin, A systematic review of the prediction of hospital length of stay: Towards a unified framework, *PLOS Digital Health* 1 (4) (2022) e0000017. doi:10.1371/journal.pdig.0000017.
URL <https://www.ncbi.nlm.nih.gov/pmc/articles/PMC9931263/>
- [39] A. Johnson, L. Bulgarelli, T. Pollard, S. Horng, L. A. Celi, R. Mark, Mimic-iv (version 2.2) (2023). doi:https://doi.org/10.13026/6mml-ek67. URL <https://physionet.org/content/mimiciv/2.2/>
- [40] L. Hempel, S. Sadeghi, T. Kirsten, Prediction of intensive care unit length of stay in the mimic-iv dataset, *Applied Sciences* 13 (12) (2023). doi:10.3390/app13126930.
URL <https://www.mdpi.com/2076-3417/13/12/6930>
- [41] WHO, Cardiovascular diseases (CVDs), [https://www.who.int/news-room/fact-sheets/detail/cardiovascular-diseases-\(cvds\)](https://www.who.int/news-room/fact-sheets/detail/cardiovascular-diseases-(cvds)), [Online] Accessed 24-April-2024 (2019).
- [42] S. S. Mahmood, D. Levy, R. S. Vasan, T. J. Wang, The framingham heart study and the epidemiology of cardiovascular disease: a historical perspective, *The lancet* 383 (9921) (2014) 999–1008. doi:10.1016/S0140-6736(13)61752-3.
URL <https://www.ncbi.nlm.nih.gov/pmc/articles/PMC4159698/>
- [43] M. K. Ali, K. I. Galaviz, M. B. Weber, K. V. Narayan, The global burden of diabetes, *Textbook of diabetes* (2017) 65–83doi:https://doi.org/10.1002/9781118924853.ch5.
- [44] X. An, Y. Zhang, W. Sun, X. Kang, H. Ji, Y. Sun, L. Jiang, X. Zhao, Q. Gao, F. Lian, et al., Early effective intervention can significantly reduce all-cause mortality in prediabetic patients: a systematic review and meta-analysis based on high-quality clinical studies, *Frontiers in Endocrinology* 15 (2024) 1294819. doi:10.3389/fendo.2024.1294819.
URL <https://www.ncbi.nlm.nih.gov/pmc/articles/PMC10941028/>
- [45] CDC - Behavioral Risk Factor Surveillance System (BRFSS), <http://www.cdc.gov/brfss/index.html>, [Online] Accessed 21 March 2022 (2015).
- [46] M. P. LaValley, Logistic regression, *Circulation* 117 (18) (2008) 2395–2399. doi:https://doi.org/10.1161/CIRCULATIONAHA.106.682658.
URL <https://www.ahajournals.org/doi/full/10.1161/circulationaha.106.682658>
- [47] S. Suthaharan, S. Suthaharan, Decision tree learning, *Machine Learning Models and Algorithms for Big Data Classification: Thinking with Examples for Effective Learning* (2016) 237–269doi:https://doi.org/10.1007/978-1-4899-7641-3_10.
- [48] S. J. Rigatti, Random forest, *Journal of Insurance Medicine* 47 (1) (2017) 31–39. doi:10.17849/inm-47-01-31-39.1.
URL <https://pubmed.ncbi.nlm.nih.gov/28836909/>
- [49] V. N. Vapnik, The nature of statistical learning theory (1995).
- [50] T. Cover, P. Hart, Nearest neighbor pattern classification, *IEEE Transactions on Information Theory* 13 (1) (1967) 21–27. doi:10.1109/TIT.1967.1053964.
URL <https://ieeexplore.ieee.org/document/1053964>
- [51] A. Mucherino, P. J. Papajorgji, P. M. Pardalos, *k*-Nearest Neighbor Classification, Springer New York, 2009, pp. 83–106. doi:https://doi.org/10.1007/978-0-387-88615-2_4.
- [52] Y. Freund, R. E. Schapire, A decision-theoretic generalization of on-line learning and an application to boosting, *Journal of Computer and System Sciences* 55 (1) (1997) 119–139. doi:https://doi.org/10.1006/jcss.1997.1504.
URL <https://www.sciencedirect.com/science/article/pii/S00220009791504X>
- [53] J. Friedman, Greedy function approximation: A gradient boosting machine, *The Annals of Statistics* 29 (11) (2000). doi:10.1214/aos/1013203451.
- [54] T. Chen, C. Guestrin, Xgboost: A scalable tree boosting system, in: *Proceedings of the 22nd ACM SIGKDD International Conference on Knowledge Discovery and Data Mining, Association for Computing Machinery*, 2016, p. 785–794. doi:10.1145/2939672.2939785.
URL <https://doi.org/10.1145/2939672.2939785>
- [55] Y. Freund, R. E. Schapire, et al., Experiments with a new boosting algorithm, in: *ICML*, Vol. 96, 1996, pp. 148–156. doi:https://dl.acm.org/doi/10.5555/3091696.3091715.
- [56] N. V. Chawla, K. W. Bowyer, L. O. Hall, W. P. Kegelmeyer, Smote: synthetic minority over-sampling technique, *Journal of artificial intelligence research* 16 (2002) 321–357. doi:https://doi.org/10.1613/jair.953.
- [57] H. He, Y. Bai, E. A. Garcia, S. Li, Adasyn: Adaptive synthetic sampling approach for imbalanced learning, in: 2008 IEEE international joint conference on neural networks (IEEE world congress on computational intelligence), IEEE, 2008, pp. 1322–1328. doi:10.1109/IJCNN.2008.4633969.
URL <https://ieeexplore.ieee.org/document/4633969>
- [58] C. Luo, Z. Duan, Z. Xia, Q. Li, B. Wang, T. Zheng, D. Wang, D. Han, Minimum heart rate and mortality after cardiac surgery: retrospective analysis of the multi-parameter intelligent monitoring in intensive care (mimic-iii) database, *Scientific Reports* 13 (02) (2023). doi:10.1038/s41598-023-29703-9.
URL <https://www.nature.com/articles/s41598-023-29703-9>
- [59] I. Weiner, W. Mitch, J. Sands, Urea and ammonia metabolism and the control of renal nitrogen excretion, *Clinical journal of the American Society of Nephrology : CJASN* 10 (2014) 1444–58. doi:10.2215/CJN.10311013.
URL <https://www.ncbi.nlm.nih.gov/pmc/articles/PMC4527031/>
- [60] M. Tonelli, F. Sacks, M. Arnold, L. Moye, B. Davis, M. Pfeffer, Relation between red blood cell distribution width and cardiovascular event rate in people with coronary disease, *Circulation* 117 (2) (2008) 163–168. doi:https://doi.org/10.1161/CIRCULATIONAHA.107.727545.
URL <https://pubmed.ncbi.nlm.nih.gov/18172029/>
- [61] S. De Rosa, M. Greco, M. Raueo, M. G. Annetta, The good, the bad, and the serum creatinine: exploring the effect of muscle mass and nutrition, *Blood Purification* 52 (9-10) (2023) 775–785.
- [62] M. A. Puskarich, U. Nandi, B. G. Long, A. E. Jones, Association between persistent tachycardia and tachypnea and in-hospital mortality among non-hypotensive emergency department patients admitted to the hospital, *Clinical and Experimental Emergency Medicine* 4 (2017) 2 – 9. doi:10.15441/ceem.16.144.
URL <https://api.semanticscholar.org/CorpusID:14065571>
- [63] B. A. Cunha, K. W. Shea, Fever in the intensive care unit, *Infectious Disease Clinics* 10 (1) (1996) 185–209.
- [64] A. C. Flint, C. Conell, X. Ren, N. M. Banki, S. L. Chan, V. A. Rao, R. B. Melles, D. L. Bhatt, Effect of systolic and diastolic blood pressure on cardiovascular outcomes, *New England Journal of Medicine* 381 (3) (2019) 243–251. doi:10.1056/NEJMoa1803180.
URL <https://www.nejm.org/doi/full/10.1056/NEJMoa1803180>
- [65] A. Poznyak, L. Litvinova, P. Poggio, V. Sukhorukov, A. Orekhov, Effect of glucose levels on cardiovascular risk, *Cells* 11 (2022) 3034. doi:10.3390/cells11193034.
URL <https://www.ncbi.nlm.nih.gov/pmc/articles/PMC9562876/>
- [66] S. A. Peters, Y. Singhathe, D. Mackay, R. R. Huxley, M. Woodward, Total cholesterol as a risk factor for coronary heart disease and stroke in women compared with men: A systematic review and meta-analysis, *Atherosclerosis* 248 (2016) 123–131.
- [67] A. Dharod, E. Z. Soliman, F. Dawood, H. Chen, S. Shea, S. Nazarian, A. G. Bertoni, M. Investigators, et al., Association of asymptomatic bradycardia with incident cardiovascular disease and mortality: the multi-ethnic study of atherosclerosis (mesa), *JAMA internal medicine* 176 (2) (2016) 219–227.
- [68] G. Gallucci, A. Tartarone, R. Lerose, A. V. Lalinga, A. M. Capobianco, Cardiovascular risk of smoking and benefits of smoking cessation, *Journal of thoracic disease* 12 (7) (2020) 3866. doi:10.21037/jtd.2020.02.47.
URL <https://www.ncbi.nlm.nih.gov/pmc/articles/PMC7399440/>
- [69] T. Tillmann, J. Vaucher, A. Okbay, H. Pikhart, A. Peasey, R. Kubinova, A. Pajak, S. Malyutina, F. Hartwig, K. Fischer, G. Veronesi, T. Palmer,

- J. Bowden, G. Smith, M. Bobak, M. Holmes, Education and coronary heart disease: Mendelian randomisation study, *BMJ* 358 (2017) j3542. doi:10.1136/bmj.j3542.
 URL <https://www.ncbi.nlm.nih.gov/pmc/articles/PMC5594424/>
- [70] C. Held, N. Hadziosmanovic, P. Aylward, E. Hagström, J. Hochman, R. Stewart, H. White, L. Wallentin, Body mass index and association with cardiovascular outcomes in patients with stable coronary heart disease – a stability substudy, *Journal of the American Heart Association* 11 (01 2022). doi:10.1161/JAHA.121.023667.
- [71] G. S. Wei, S. A. Coady, D. C. Goff Jr, F. L. Brancati, D. Levy, E. Selvin, R. S. Vasan, C. S. Fox, Blood pressure and the risk of developing diabetes in african americans and whites: Aric, cardia, and the framingham heart study, *Diabetes care* 34 (4) (2011) 873–879. doi:10.2337/dc10-1786.
 URL <https://www.ncbi.nlm.nih.gov/pmc/articles/PMC3064044/>
- [72] E.-J. Rhee, K. Han, S.-H. Ko, K.-S. Ko, W.-Y. Lee, Increased risk for diabetes development in subjects with large variation in total cholesterol levels in 2,827,950 koreans: A nationwide population-based study, *PLOS ONE* 12 (2017) e0176615. doi:10.1371/journal.pone.0176615.
 URL <https://www.ncbi.nlm.nih.gov/pmc/articles/PMC5436642/>
- [73] E. S. of Cardiology, Body mass index is a more powerful risk factor for diabetes than genetics, *ScienceDaily* (2020).
 URL www.sciencedaily.com/releases/2020/08/200831090129.htm
- [74] L. DiPietro, D. Buchner, D. Marquez, R. Pate, L. Pescatello, M. Whitt-Glover, New scientific basis for the 2018 u.s. physical activity guidelines, *Journal of Sport and Health Science* 8 (2019) 197–200. doi:10.1016/j.jshs.2019.03.007.
 URL <https://www.ncbi.nlm.nih.gov/pmc/articles/PMC6525104/>
- [75] K. Sil, B. K. Das, S. Pal, L. Mandal, A study on impact of education on diabetic control and complications, *National Journal of Medical Research* 10 (01) (2020) 26–29.
 URL <https://njmr.in/index.php/file/article/view/48>
- [76] Diabetes, UK, Cardiovascular Disease and Diabetes, https://www.diabetes.org.uk/guide-to-diabetes/complications/cardiovascular_disease, [Online] Accessed April 15, 2024 .
- [77] S. Verma, V. Boonsanong, M. Hoang, K. E. Hines, J. P. Dickerson, C. Shah, Counterfactual explanations and algorithmic recourses for machine learning: A review (2022). arXiv:2010.10596, doi:https://doi.org/10.48550/arXiv.2010.10596.
- [78] S. B. Mushlin, H. L. Greene, Decision making in medicine: an algorithmic approach, *Elsevier Health Sciences*, 2009. doi:10.1016/S0377-1237(02)80153-8.